CHAPTER IV

RESULTS AND DISCUSSION

In the present study on the hydrodesulfurization of gas oil catalyzed by *in situ* molybdenum compounds, the experiments were divided into:

1. To synthesize of tetrabutylammonium thiomolybdate (TBATM) precursor.
2. To characterize *in situ* generated MoS_2 catalysts from ATM and TBATM precursors with and without cobalt promoter.
3. To study the hydrodesulfurization of sulfur model compounds and real oil feedstocks catalyzed by *in situ* generated MoS_2 catalysts.

The results of the experiments are described as follows:

4.1 Synthesis of tetrabutylammonium thiomolybdate (TBATM)

In this work, tetrabutylammonium thiomolybdate (TBATM) was synthesized in high yield (72.7%) by the following reaction:

$$(NH_4)_2MoS_4 + 2[CH_3(CH_2)_3]_4N^+Br^- \xrightarrow{H_2O} ([CH_3(CH_2)_3]_4N)_2MoS_4 + NH_4Br + H_2O \quad (4.1)$$

This compound was characterized by ^1H NMR and ^{13}C NMR, the spectra were shown in Figures 4.1 – 4.2.

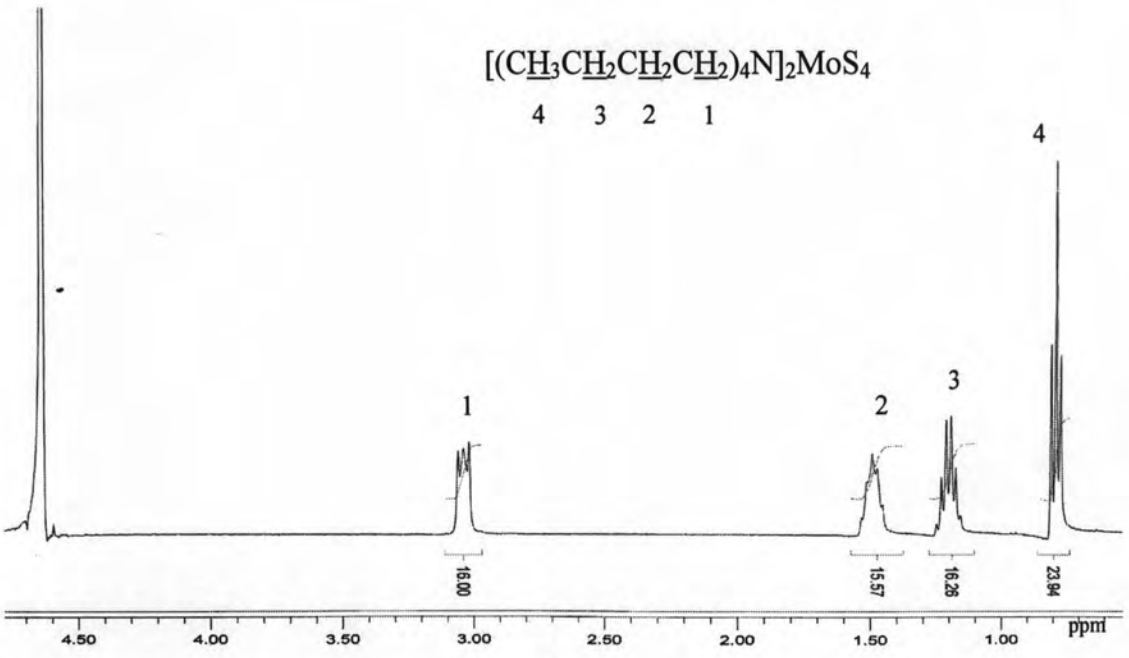

Figure 4.1 ^{1}H NMR spectrum of TBATM precursor.

Figure 4.1 shows the ^{1}H NMR spectrum of TBATM which consists of four signals coming from four different types of protons. The first signal corresponds to a triplet at δ_H 3.04 (t, J = 8.4 Hz) due to 16 protons in CH_2 groups connecting with the N atom. The next two multiplet signals at δ_H 1.21 and 1.49 are attributed to 16 protons of CH_2 groups connecting with CH_2-N and CH_3 groups, respectively. Finally, the triplet signal at δ_H 0.78 (t, J = 7.3 Hz) is provided by 24 protons assigned to CH_3 groups. The ^{1}H NMR result of TBATM is in good agreement with previous report [27].

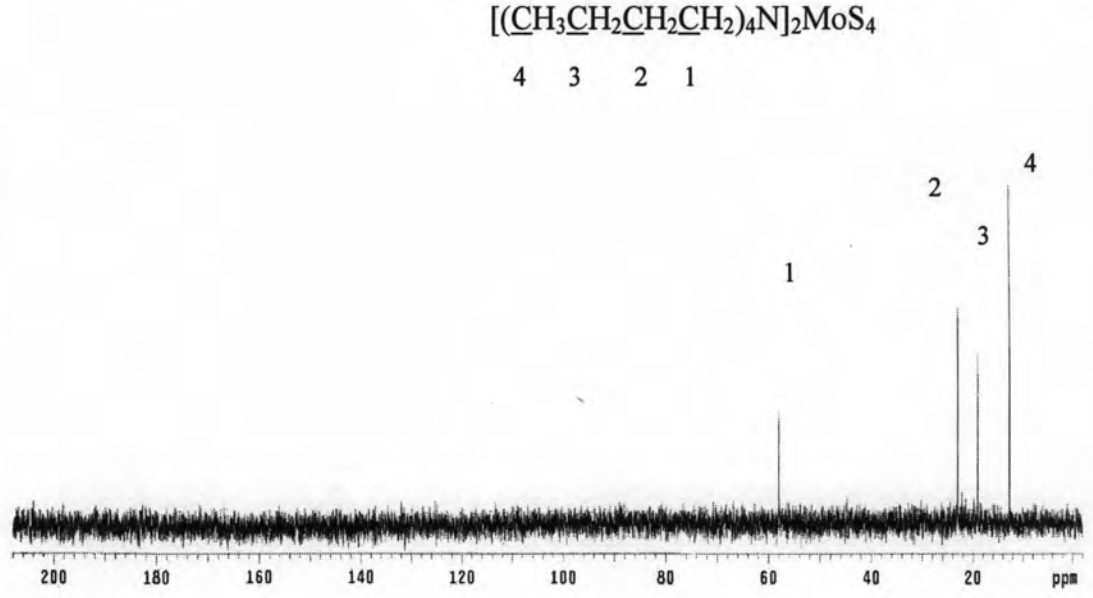

Figure 4.2 ^{13}C NMR spectrum of TBATM precursor.

Figure 4.2 shows the ^{13}C NMR of TBATM. The peak at δ_C 58 is ascribed to the CH_2 next to the nitrogen atom. The peaks at δ_C 19 and 23 are attributed to the continuing CH_2 groups as their positions become farther from the N atom. The peak at δ_C 12 belongs to the CH_3 group.

4.2 Thermal analysis of thiomolybdate precursor

Thermogravimetric (TGA) was used to characterize the thermal decomposition of ammonium thiomolybdate (ATM) and tetrabutylammonium thiomolybdate (TBATM).

4.2.1 TGA of ammonium tetrathiomolybdate precursor (ATM)

The thermogravimetric (TGA) curve for ATM precursor under N_2 was shown in Figure 4.3.

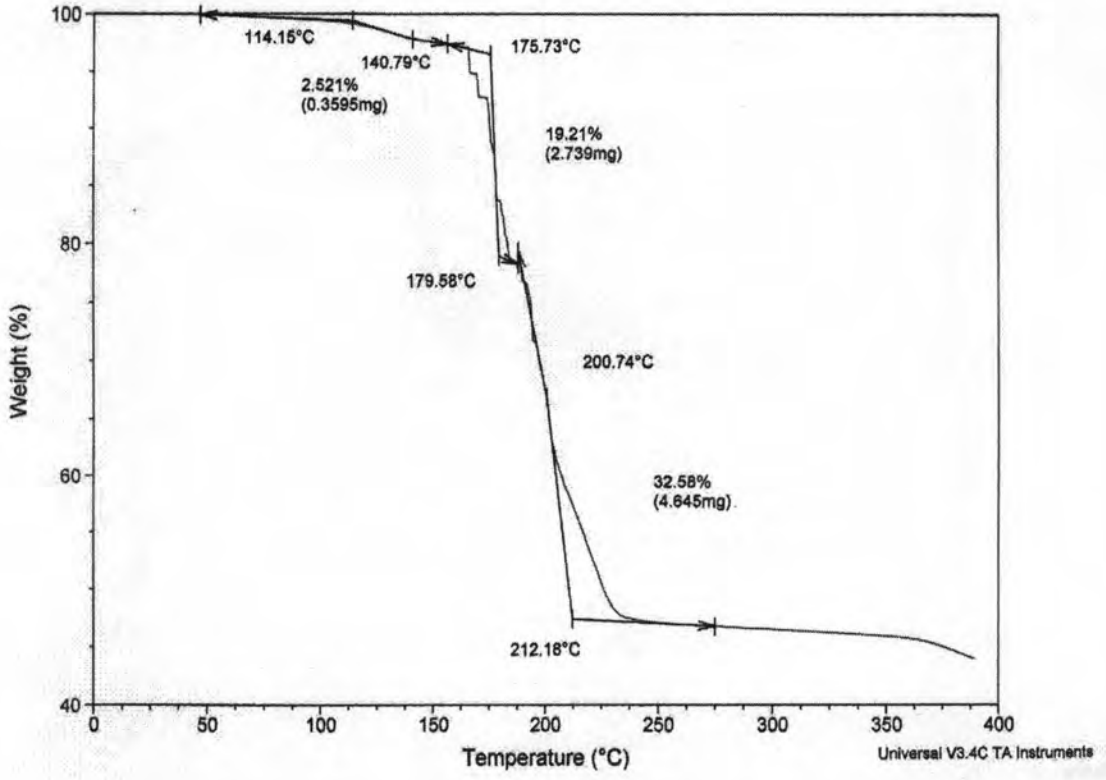

Figure 4.3 TGA curve of the decomposition of ATM precursor under N_2.

The decomposition of the ATM precursor present two steps of decomposition:

1. The first decomposition step in the temperature region 175 – 179 °C with a weight loss of 19.21% as a sharp step that corresponds to the loss of ammonia and hydrogen sulfide, according to the reaction

$$(NH_4)_2MoS_4 \longrightarrow 2NH_3 + H_2S + MoS_3 \qquad (4.3)$$

2. The second decomposition step in the temperature region 200 – 212 °C was found to be 32.58% weight loss. Molybdenum trisulfide thus generated decompose with the simultaneous reduction of Mo^{+6} to Mo^{+4} and oxidation of S^{2-} to S^0

$$MoS_3 \longrightarrow MoS_2 + S \qquad (4.4)$$

This result agrees with that reported in the literature [33] which indicated that thermal decomposition of ATM gave ammonia (NH_3) and hydrogen sulfide (H_2S) at 150 – 220 °C to form MoS_3. The second decomposition step is around 150 – 220 °C.

However, it is important to note that final composition of MoS_2 depends on the type of atmosphere during the thermal decomposition of the thiosalt.

In the *in situ* experiments, the set temperature of the reactor (350 °C) corresponds to the lower limit of the decomposition temperature for the second step (decomposition of MoS_3 to MoS_2 + S), and sulfur-rich MoS_{2+x} phase may be expected. Intermediate compounds showing S/Mo stoichiometries from 2.4 to 2.7 have been reported in the literature [28]. However, amorphous MoS_3 is very sensitive to the presence of hydrogen, which lowers the onset of its decomposition [29].

4.2.2 TGA of tetrabutylammonium thiomolybdate precursor (TBATM)

Figure 4.4 shows the resultant thermogravimetric TGA curve for TBATM precursor under N_2.

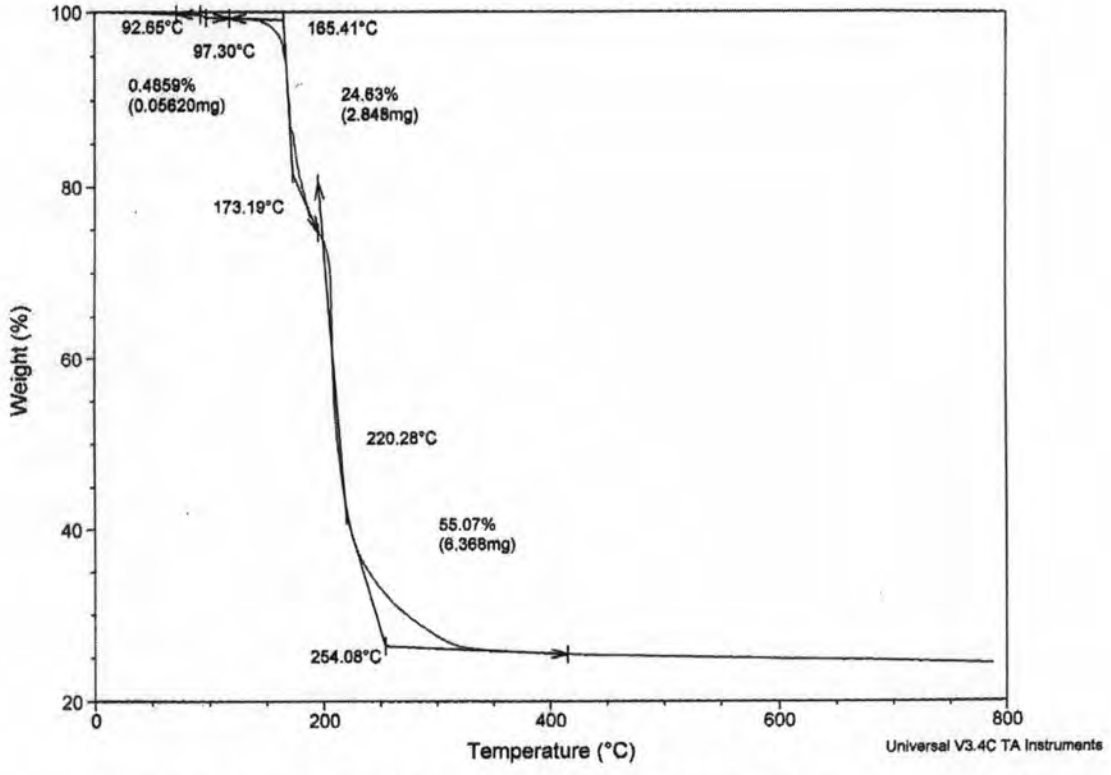

Figure 4.4 TGA curve of the decomposition of TBATM precursor under N_2.

From the TGA curve, the appearance of the first small step (0.48% of weight loss) in the thermogram of TBATM precursor seems due to the elimination of water.

Since these materials were crystallized from a saturated aqueous solution, some amount of water can be expected to contaminate the thiosalts. An early-run weight-loss has been ascribed to the dehydration of the starting materials [34].

Two steps of weight loss are distinguishable from the thermal decomposition of the TBATM precursors, these transitions are consistent with the following series of reactions:

1. The first decomposition occurs in the temperature region 165 – 173 °C with a weight loss of 24.63%, this was proposed to involve elimination of tributylamine $[CH_3(CH_2)_3]_3N$ and butylamine sulfide $CH_3(CH_2)_3N{=}S$.

$$\{[CH_3(CH_2)_3]_4N\}_2MoS_4 \longrightarrow [CH_3(CH_2)_3]_3N + CH_3(CH_2)_3NS + [CH_3(CH_2)_3]_4MoS_3 \quad (4.5)$$

2. The second step occurs in the temperature region 220 – 254 °C with a weight loss of 55.07%, this suggested the elimination of dibutylsulfide $[CH_3(CH_2)_3]_2S$ and octane $[CH_3(CH_2)_6CH_3]$.

$$[CH_3(CH_2)_3]_4MoS_3 \longrightarrow [CH_3(CH_2)_3]_2S + CH_3(CH_2)_6CH_3 + MoS_2 \quad (4.6)$$

The final product of the thermal decomposition correspond to MoS_2. This complicate decomposition pattern involved intramolecular rearrangement and interaction with neighboring units of TBATM. The resulting TGA curve for tetrabutylammonium thiomolybdate is in agreement with those reported [35].

In summary, it was found that by *in situ* decomposition of ammonium tetrathiomolybdate (ATM) and tetrabutylammonium thiomolybdate (TBATM) precursors, unsupported MoS_2 catalysts can be synthesized.

In this work, unsupported MoS_2 catalysts were synthesized from ammonium tetrathiomolybdate (ATM) and tetrabutylammonium thiomolybdate (TBATM) precursors by *in situ* decomposition during the hydrodesulfurization (HDS) of dibenzothiophene (DBT) and 4,6-dimethhyldibenzothiophene (4,6-DMDBT) as sulfur

model compounds and straight run gas oil (SRGO) and light cycle oil (LCO) as real oil feedstocks. *In situ* generated MoS_2 catalysts from ATM and TBATM precursors obtained *in situ* activation without substrate and after HDS reaction were characterized with XRD, BET, EDX and SEM.

4.3 Characterization of *in situ* generated MoS_2 and Co/MoS_2 catalysts

Characterization of *in situ* generated MoS_2 and Co/MoS_2 catalysts were performed on samples obtained *in situ* activation without substrate and recovered after the hydrodesulfurization.

4.3.1 X-ray diffraction (XRD)

The structures characteristic of the *in situ* generated MoS_2 catalysts were investigated by XRD technique. The XRD patterns of *in situ* generated MoS_2 catalysts from ATM and TBATM with and without added water obtained *in situ* activation without substrate and after HDS reaction were shown in Figures 4.5 and 4.6, respectively.

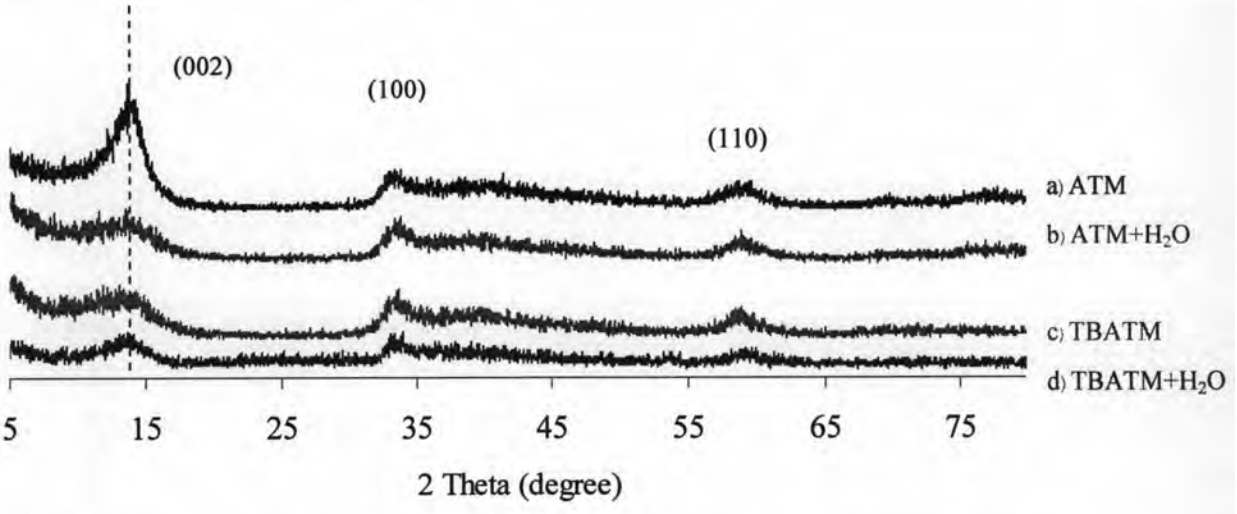

Figure 4.5 XRD patterns of *in situ* generated MoS_2 catalysts (obtained *in situ* activation without substrate).

Figure 4.5 shows the XRD patterns of the *in situ* generated MoS_2 catalysts from ATM and TBATM precursors (obtained *in situ* activation without substrate). All these patterns showed poorly crystalline structure of MoS_2 (JCPDS-ICDD 3701492) with the characteristic peaks at 2θ (Å) = 14° (002), 33(100) and 58(110) in agreement with those reported [36].

From comparative examination according to the diffraction patterns in Figure 4.5, it becomes clear that *in situ* generated MoS_2 catalyst from ATM and ATM+H_2O have similar XRD patterns, suggested that the samples prepared from ATM+H_2O is MoS_2 like material. However, the (002) peak of the latter is broader and decrease in intensity while other peaks remain the same, when added water to the reaction, indicating that layer stacking of MoS_2 is affected. The very weak (002) peak suggests that the degree of MoS_2 layer stacking is much smaller in the *in situ* generated MoS_2 catalyst from ATM+H_2O than in the *in situ* generated MoS_2 from ATM [36].

Compared between ATM and TBATM, the (002) signal indicates a marked decrease in the stacking along the *c* direction when an alkyl group is incorporated to the precursor. This suggests a possible exfoliating effect when large amounts of carbon are generated during the *in situ* decomposition of TBATM [37].

In the case of TBATM, XRD patterns of *in situ* generated MoS_2 catalysts from TBATM and TBATM+H_2O show similar pattern with that from ATM+H_2O. However, a slight increase in intensity of the (002) peak is observed for MoS_2 prepared from TBATM and TBATM+H_2O.

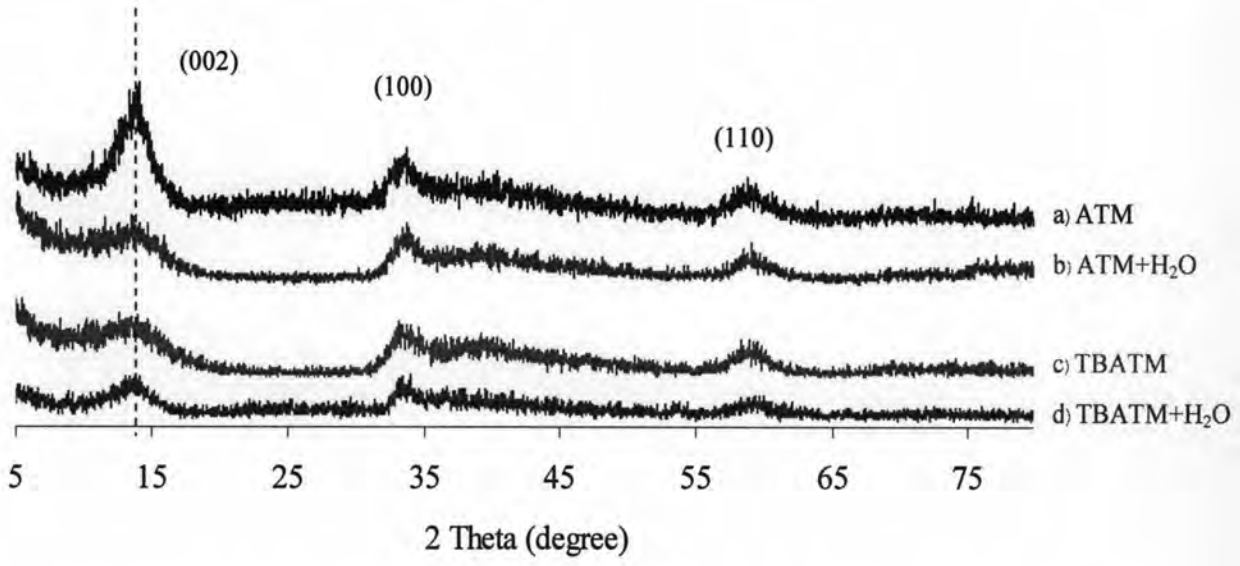

Figure 4.6 XRD patterns of *in situ* generated MoS_2 catalysts (after HDS reaction).

Figure 4.6 shows the XRD patterns of the *in situ* generated MoS_2 catalysts from ATM and TBATM precursors after HDS reaction. All patterns present weak peaks corresponding to a very poorly crystallite structure characteristic of MoS_2. All these patterns show similar pattern of MoS_2 catalysts obtained *in situ* activation without substrate (Figure 4.5). The XRD results after HDS reaction confirmed that *in situ* generated MoS_2 catalysts from ATM and TBATM precursors with and without added water prepared from *in situ* activation without substrate and after HDS reaction obtained to final MoS_2 catalysts.

For the cobalt promoted with ATM and TBATM precursors. The XRD patterns of *in situ* generated Co/MoS_2 catalysts from ATM and TBATM with and without added water were shown in Figures 4.7 and 4.8.

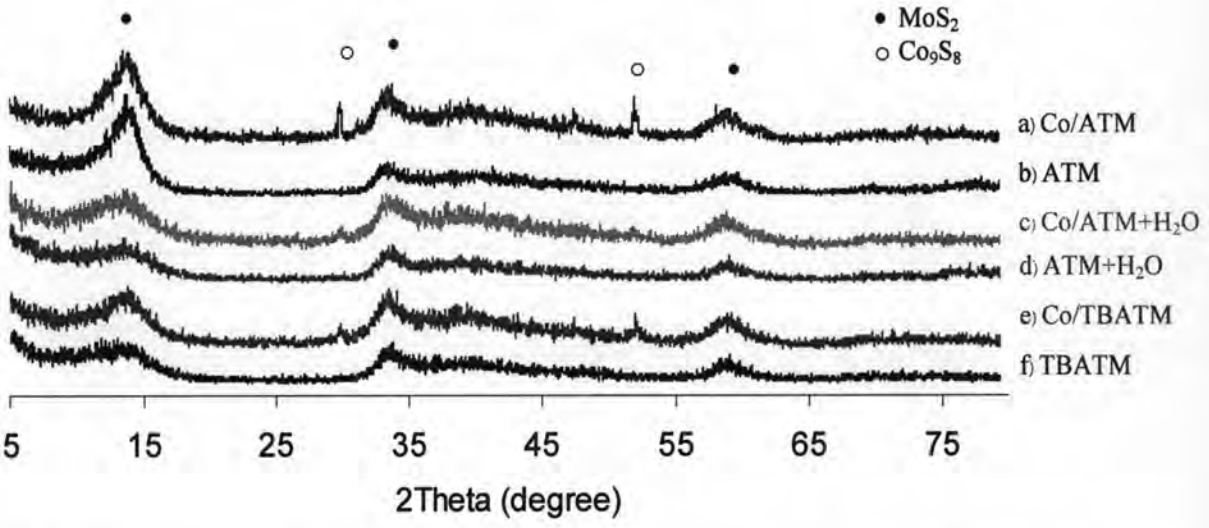

Figure 4.7 XRD patterns of *in situ* generated MoS_2 and Co/MoS_2 catalysts (obtained *in situ* activation without substrate).

According to the diffraction pattern in Figure 4.7, when promoted with cobalt, all these patterns of *in situ* generated Co/MoS_2 catalysts from ATM and TBATM precursors still exhibited poorly crystalline structure of MoS_2 (JCPDS-ICDD 3701492), peak at 2θ (Å) = 14° (002), 33(100), 40(103) and 58(110), together with the cobalt sulfide phase.

As reported in the literature [38], in the sulfide form, cobalt may be present as Co_9S_8 crystallites, when cobalt ions adsorbed onto the surface of MoS_2 crystallites Though some Co-Mo sulfides with well-defined structure were described in the literature [39], the most catalytically active Co-Mo-S species have no definite structure. It was believed that the active form exists as 'CoMoS' phase contains MoS_2 fringes, in which Co atoms are located at the edges, replacing Mo [40].

As shown in figure 4.7, XRD patterns of *in situ* generated Co/MoS_2 catalysts from $ATM+H_2O$ present very weak in intensity of peaks of cobalt sulfide phase, suggesting that promoter atoms are well dispersed on the active phase [41]. In addition, the data from EDX analysis (section 4.3.2, Table 4.1) show that *in situ* generated Co/MoS_2 catalysts from ATM+Coacetate exhibits Co/Mo ratio of 0.12 while Co/MoS_2 catalyst from $ATM+H_2O$+Coacetate shows the ratio of Co/Mo ratio 0.36, confirming that cobalt sulfide are well dispersed on the active phase.

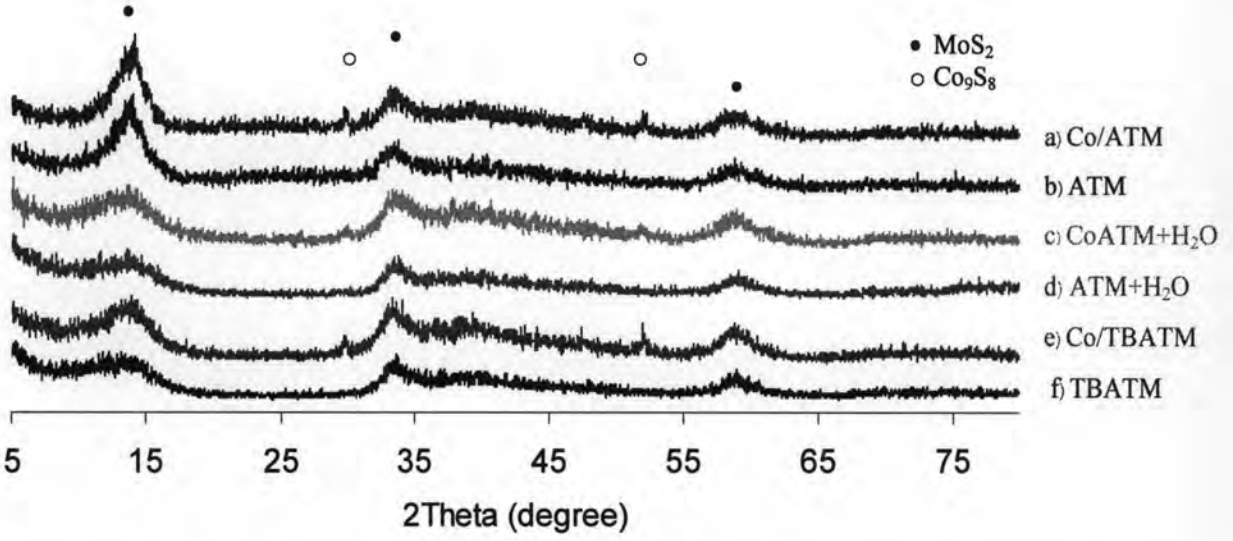

Figure 4.8 XRD patterns of *in situ* generated MoS_2 and Co/MoS_2 catalysts (after HDS reaction).

The diffractograms of *in situ* generated MoS_2 catalysts after HDS reaction are presented in Figure 4.8. The XRD patterns of the *in situ* generated Co/MoS_2 catalysts from ATM and TBATM precursors with and without added water after HDS reaction. All these patterns show similar pattern of *in situ* Co/MoS_2 catalysts obtained *in situ* activation without substrate (Figure 4.7). The XRD results after HDS reaction confirmed that *in situ* generated Co/MoS_2 catalysts from ATM and TBATM precursors with and without cobalt promoter prepared from *in situ* activation without substrate and after HDS reaction obtained to final Co/MoS_2 catalysts.

Intensities of these cobalt sulfide species decreased in XRD patterns after HDS reaction indicating a redispersion of cobalt. This is in good agreement with the results of previous report in which intensities of nickel sulfide decreased in XRD patterns after HDS of DBT [42].

4.3.2 Surface area and total pore volume

BET specific surface area for the *in situ* generated MoS_2 and Co/MoS_2 catalyst from ATM and TBATM precursors with and without added water were measured from *in situ* activation without substrate and after HDS reaction. The results are summarized in Table 4.1.

Table 4.1 Specific surface area and total pore volume of *in situ* generated MoS_2 and Co/MoS_2 catalysts obtained *in situ* activation without substrate and after HDS reaction.

In situ MoS_2 catalyst	Surface area (m^2/g)	Pore volume (cm^3/g)	Elemental analysis
In situ activation without substrate*			
ATM	120	0.18	$MoS_{1.8}C_{4.7}$
ATM + H_2O	544	1.16	$MoS_{1.7}C_{8.9}$
ATM + Coacetate	77	0.14	$MoS_{1.8}Co_{0.12}C_{2.4}$
ATM + H_2O + Coacetate	146	0.53	$MoS_{2.1}Co_{0.36}C_{5.3}$
TBATM	270	0.23	$MoS_{1.6}C_{3.8}$
TBATM + H_2O	83	0.12	$MoS_2C_{2.9}$
TBATM + Coacetate	219	0.37	$MoS_2Co_{0.3}C_{3.5}$
After HDS reaction			
ATM	111	0.15	$MoS_{1.6}C_{5.4}$
ATM + H_2O	332	0.63	$MoS_{1.6}C_{7.1}$
ATM + Coacetate	68	0.14	$MoS_{1.6}Co_{0.1}C_{4.8}$
ATM + H_2O + Coacetate	122	0.45	$MoS_{2.2}Co_{0.36}C_{5.6}$
TBATM	105	0.17	$MoS_{1.3}C_{2.7}$
TBATM + H_2O	48	0.12	$MoS_{1.8}C_{2.3}$
TBATM + Coacetate	183	0.36	$MoS_{1.8}Co_{0.1}C_{2.7}$

*A new batch of freshedly prepared sample which was stored in decalin solvent and vacumm-dried before use for BET.

The results of BET analysis for all *in situ* generated MoS_2 catalysts are shown in Table 4.1, which indicates that the freshly *in situ* generated MoS_2 catalyst prepared from ATM+H_2O (under H_2 pressure 30 atm at 350 °C) have much higher surface area and the total pore volume (544 m^2/g, 1.16 cm^3/g) than those from ATM alone (120 m^2/g, 0.18 cm^3/g), which is about 5 times that of the surface area of sample from ATM without water.

Therefore, it is clear that water addition led to a high-surface area, highly active MoS_2 catalyst when used ATM as precursor. This is in a good agreement with previous reported [43].

In the case of TBATM precursor, butyl group present in TBATM precursor as carbon-containing precursor in TBATM has a direct influence on surface area and total pore volume. The result shows that TBATM marked increase in both the surface area from 111 to 270 m^2/g and the total pore volume from 0.18 to 0.32 cm^3/g. However, addition of water has a negative effect on surface area of *in situ* generated MoS_2 catalyst from TBATM precursor, *in situ* generated MoS_2 catalyst from TBATM+H_2O have very less higher surface area and total pore volume (83 m^2/g, 0.12 cm^3/g) than those from TBATM alone (270 m^2/g, 0.23 cm^3/g).

The relative range of surface area as a function of precursors was: ATM+H_2O > TBATM > ATM > TBATM+H_2O. Anyway, in the case of ATM precursor, addition of water seems to be an effective alternate that can be used to modify the structural properties of the *in situ* generated MoS_2 catalysts.

The BET surface area of *in situ* generated MoS_2 catalysts decreased considerably after HDS reaction, as shown in Table 4.1. It was evident that carbon deposits were responsible for the decrease in the surface area. Possibly, the deposited carbonaceous material was able to dispersed on the porous of MoS_2 catalyst [44]. Additionly, the decrease of surface area was attributed to sintering of MoS_2 crystallites [45].

For the cobalt promoted ATM and TBATM precursors, cobalt promotion leads to a decrease in surface area compared to the non-promoted MoS_2 catalysts. The

BET result of *in situ* generated Co/MoS_2 catalyst from ATM in a good agreement with previous reported [46], that prepared mixed sulfide from the fluxes of nickel and cobalt chloride and liquid sulfur, the prepared Co/MoS_2 catalyst had very low surface areas (75 m^2/g). Indeed, the cobalt sulfide phase was observed in the *in situ* generated Co/MoS_2 catalyst could be the reason of the low value of surface area [47].

From the results in Table 4.1, showed the different relative range of surface area between *in situ* generated of Co/MoS_2 catalysts and non-promoted MoS_2 catalysts: TBATM+Coacetate (219 m^2/g) > ATM+H_2O+Coacetate (146 m^2/g) > ATM+Coacetate (77 m^2/g).

4.3.3 Elemental analysis (EDX)

The C/Mo, S/Mo, and Co/Mo atomic ratios determine using energy dispersive x-ray (EDX) are also reported in Table 4.1 (Section 4.3.2). The S/Mo ratios for all catalysts varied from 1.7 – 2.1. EDX analysis reveals high C/Mo ratios (2.9 – 8.9) for all *in situ* generated MoS_2 catalysts from ATM and TBATM with and without added water. Especially, *in situ* generated MoS_2 catalysts from ATM+H_2O presents the highest C/Mo ratios at 8.9.

These results are comparable to those reported [48] for MoS_2 catalysts, which show MoS_xC_y is described as that of the stabilized catalyst. In addition, the evidence of the existence of carbon in the MoS_2 catalyst was reported using Auger spectroscopy [49]. The MoS_2 catalysts synthesized from decomposition of tetraalkylammonium thiomolybdate precursors, with hydrocarbon solvent (decalin) produces MoS_xC_y material on the surface, sulfur atoms are replaced by carbon, leading to stabilized sulfur-deficient carbon-containing MoS_xC_y catalysts. It is possible that surface carbon is included in the arrangement of active sites, with a promoting effect.

It has been shown recently that molybdenum carbide (Mo_2C/Al_2O_3) catalyst, produced by carburizing alumina-supported ammonium molybdate in a CH_4/H_2 reactant stream, has three times greater HDS activity than a MoS_2/Al_2O_3 catalyst [50].

For cobalt promoted MoS_2 catalyst, the *in situ* generated Co/MoS_2 catalyst from ATM, ATM+H_2O and TBATM also reveals high amount of carbon ($2.4 \leq C/Mo \geq 5.3$). Formation of sulfocarbide phase was reported for the *in situ* generated Co/MoS_2 from bimetallic alkylthiomolybdates precursors [51].

The C/Mo ratio for all catalysts measured after HDS reaction are higher than before HDS reaction. It indicates that the high amount of residual carbon may be present in the structure and also on the surface of catalysts [52].

In the case of ATM and TBATM precursors promoted with cobalt compound. The Co/Mo atomic ratio for all *in situ* generated Co/MoS_2 catalysts where as the S/Mo ratio varied from 1.8 to 2.1.

Compared with ATM and ATM+H_2O precursors promoted with cobalt compound, Co/Mo atomic ratio for *in situ* generated Co/MoS_2 catalyst from ATM = 0.1, while from ATM+H_2O = 0.36. In the preparation of CoMoS, the increase in dispersion of Mo species will increase the dispersion of Co species [37].

Although the possibility that an oxygen-containing sulfide MoO_xS_y may be the more active material may cannot be ruled out at the present stage, according to the previous report [30], it was declared that XPS indicates the oxygen content for the *in situ* generated MoS_2 catalyst from ATM+H_2O is considerably less than that from ATM, despite the addition of H_2O. The chemical analysis of the *in situ* generated MoS_2 catalysts from ATM and ATM+H_2O give S-to-Mo atomic ratios of 2.03 – 2.04, identical to that of the commercially available MoS_2 reagent.

4.3.4 N_2 adsorption-desorption isotherms and BJH pore size distributions

The N_2 adsorption-desorption isotherms and BJH pore size distributions for *in situ* generated MoS_2 catalysts from ATM and TBATM with and without added water are predicted in Figures 4.9 – 4.12.

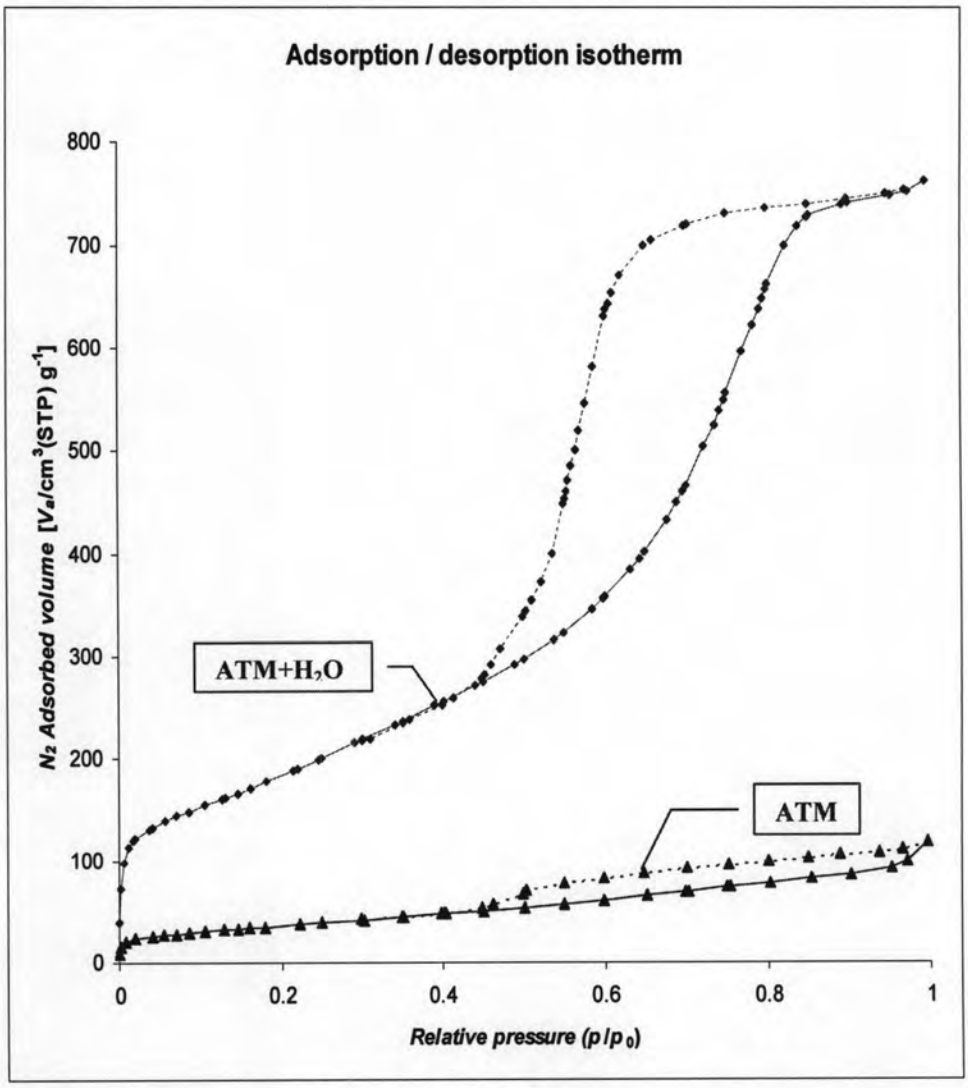

Figure 4.9 Adsorption-desorption isotherms for *in situ* generated MoS_2 catalysts from ATM and ATM+H_2O.

As observed in Figure 4.9, the adsorption-desorption curves of *in situ* generated MoS_2 catalysts from ATM and ATM+H_2O correspond to type IV isotherms with desorption curves characteristic of mesoporous materials above the relative pressure of 0.4.

For *in situ* generated MoS_2 catalyst from ATM shows a very poorly developed porous system is observed with a surface area of only 120 m^2/g. Very low values of N_2 adsorption were observed at low P/P_0 values. While *in situ* generated MoS_2 catalyst from ATM+H_2O, presents the highest surface area, it shows highest pore volume 1.16 indicating that mesoporosity contributes to a large extent to its high surface area. Indeed, this solid has the highest nitrogen adsorption values at low relative pressures P/P_0.

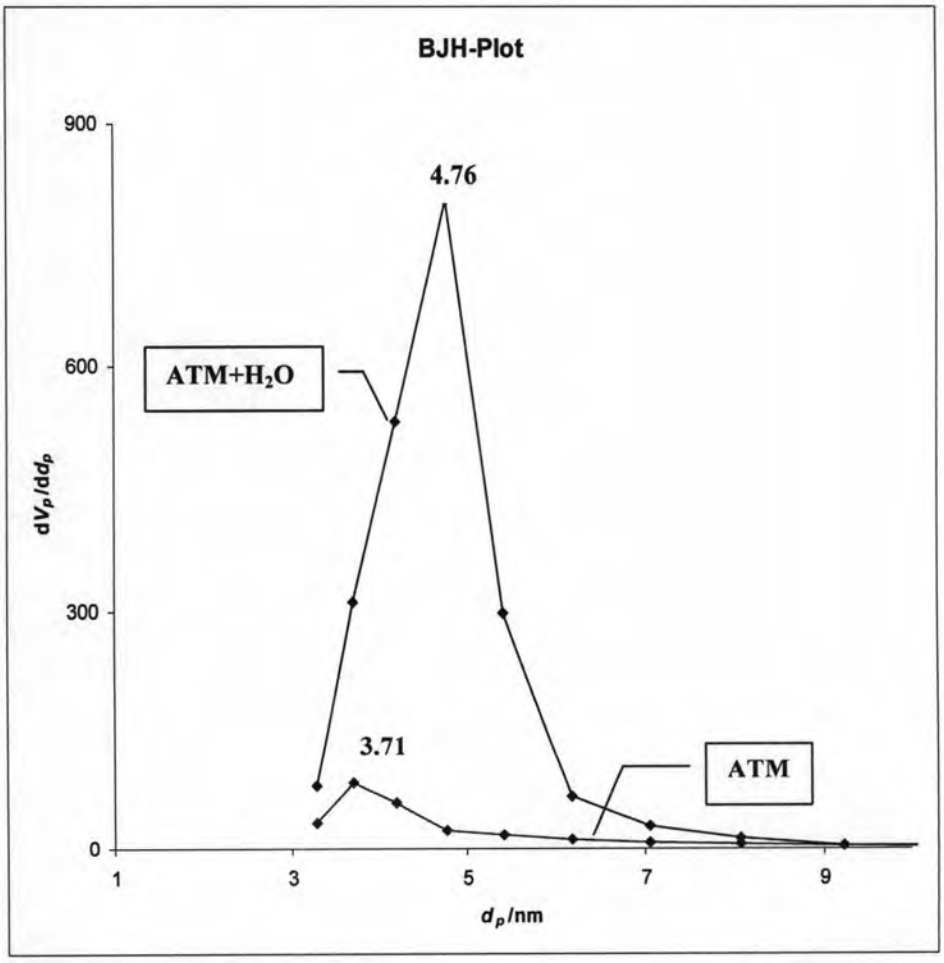

Figure 4.10 BJH pore size distributions of *in situ* generated MoS_2 catalysts from ATM and ATM+H_2O.

Figure 4.10 shows the desorption BJH pore size distributions observed for *in situ* generated MoS_2 catalyst from ATM and ATM+H_2O. The results present narrow pore size distribution, ranging from 3 to 6 nm., the mean pore size value for *in situ* generated MoS_2 catalyst from ATM is 3.71 nm, while the mean pore size for MoS_2 catalyst from ATM+H_2O shifts upward, to 4.76 nm.

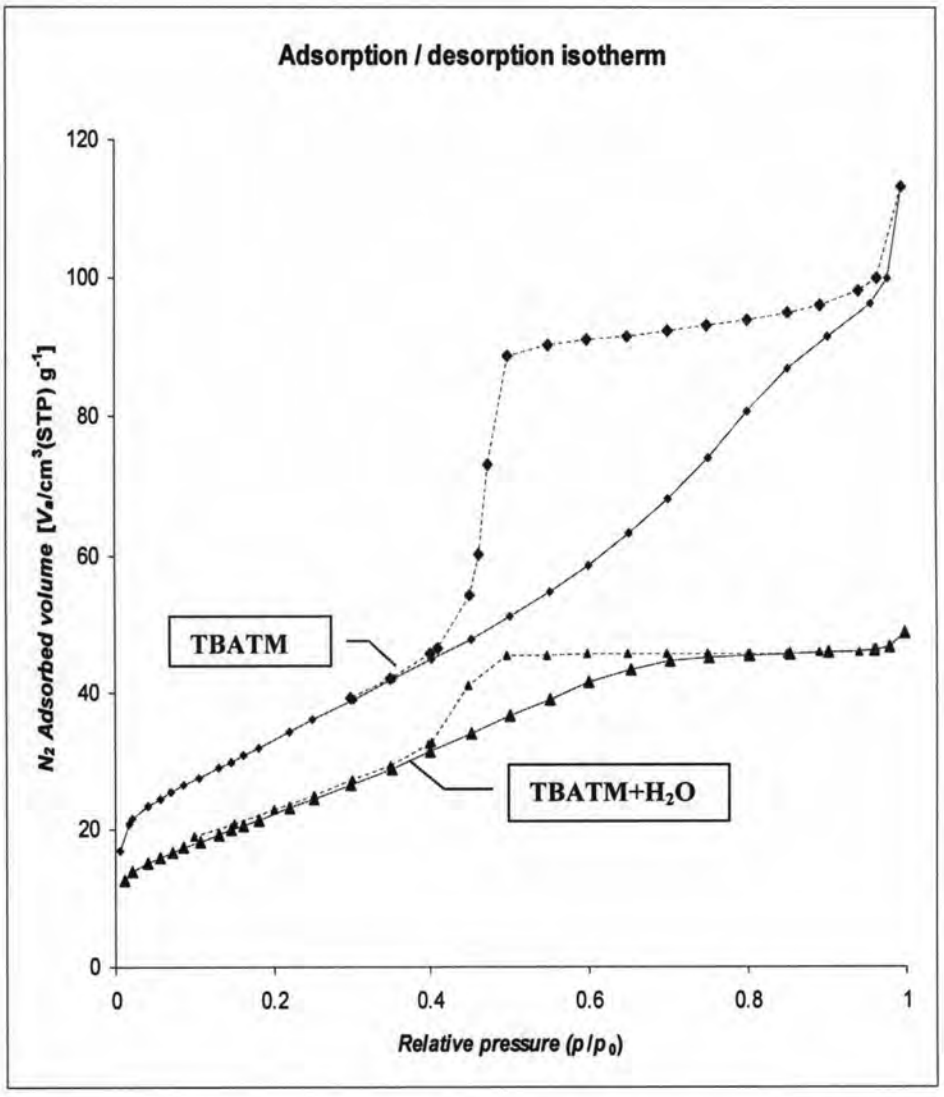

Figure 4.11 Adsorption-desorption isotherms for *in situ* generated MoS_2 catalysts from TBATM and TBATM+H_2O.

N_2 adsorption-desorption isotherms of *in situ* generated MoS_2 catalysts from TBATM and TBATM+H_2O are shown in Figure 4.11. From both isotherms present type IV isotherms, suggests that the development of a mesoporous organization at the expense when present butyl group. The hysteresis loop shown by all these materials suggest that cylindrical pores are open at both ends.

It has been reported in the literature [54] that MoS_2 catalysts derived from tetraalkylamomonium thiomolybdates, mesoporous cavities are formed because of the accumulation of gases during the escape of such gases to the exterior. Such a porous network in amorphous materials may be considered equivalent to the porous structure of molecular sieves, which very likely induce confinement effects.

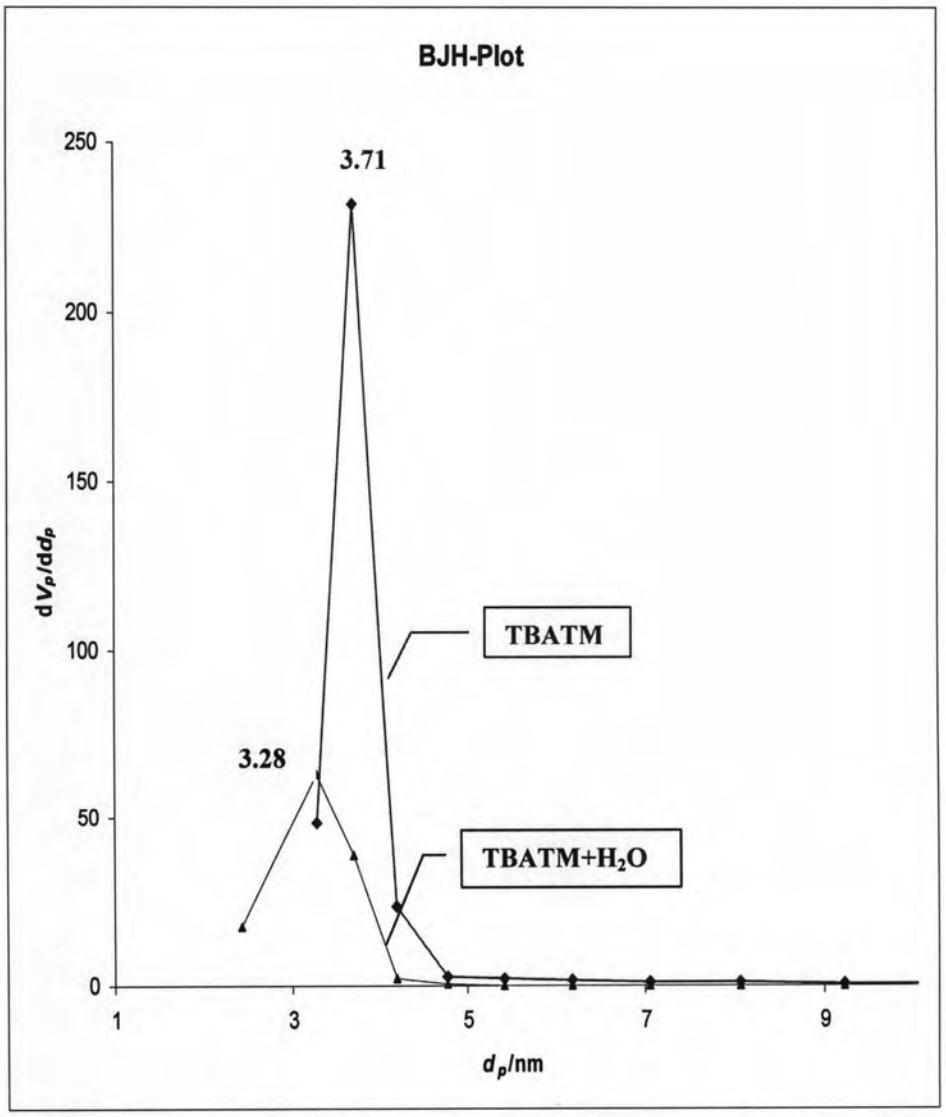

Figure 4.12 BJH pore size distributions of *in situ* generated MoS_2 catalysts from TBATM and TBATM+H_2O.

The BJH pore size distributions of *in situ* generated MoS_2 catalysts from TBATM and TBATM+H_2O. A narrow pore size distributions centered on a diameter of 3.71 nm was observed for *in situ* generated MoS_2 catalysts from TBATM, while the *in situ* generated MoS_2 catalysts from TBATM+H_2O has pore diameter of 3.28 nm.

The N_2 adsorption-desorption isotherms and BJH pore size distributions for *in situ* generated Co/MoS_2 catalysts from ATM and TBATM with and without added water are predicted in Figures 4.13 – 4.17.

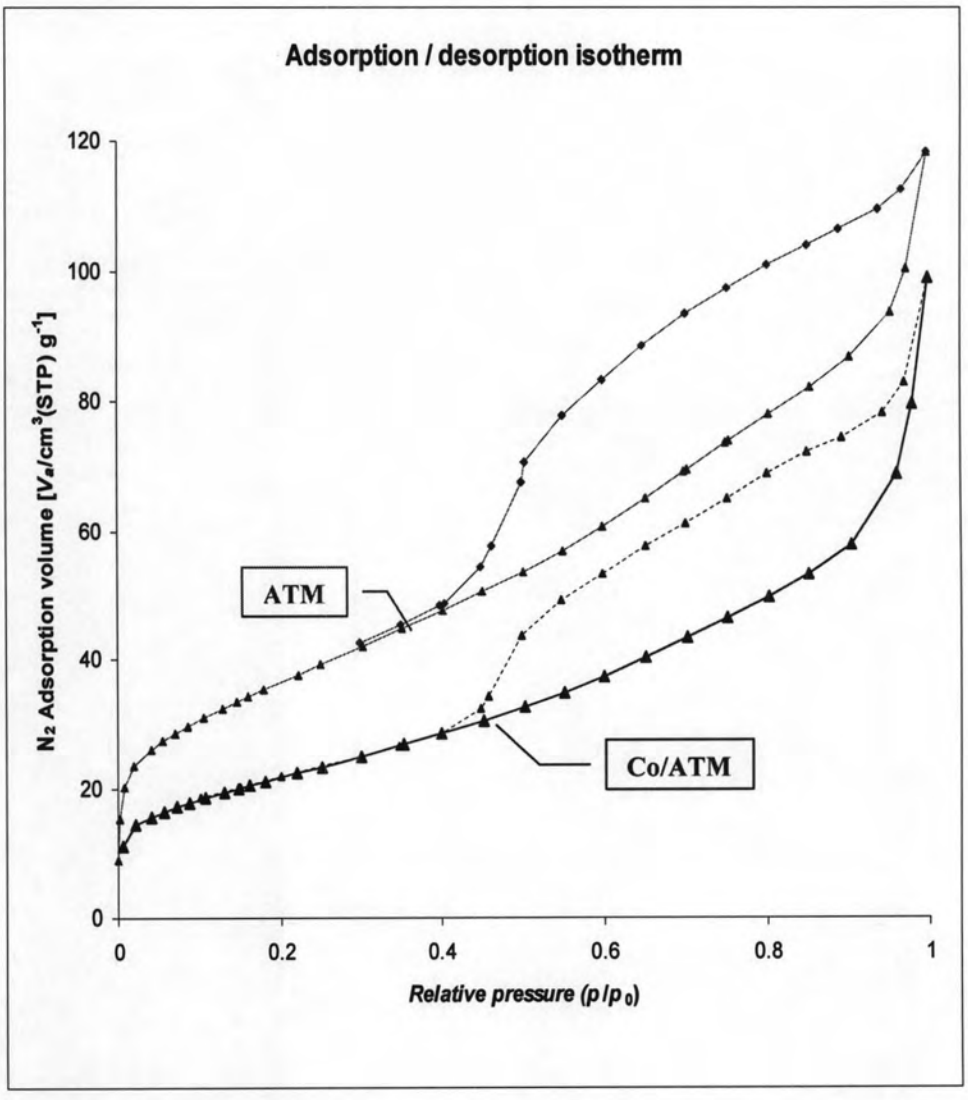

Figure 4.13 Adsorption-desorption isotherms for *in situ* generated MoS_2 and Co/MoS_2 catalysts from ATM.

Figure 4.13 presents the adsorption-desorption isotherms of *in situ* generated MoS_2 and Co/MoS_2 catalysts from ATM. These catalysts show type IV isotherms, with desorption curves characteristic of mesoporous materials.

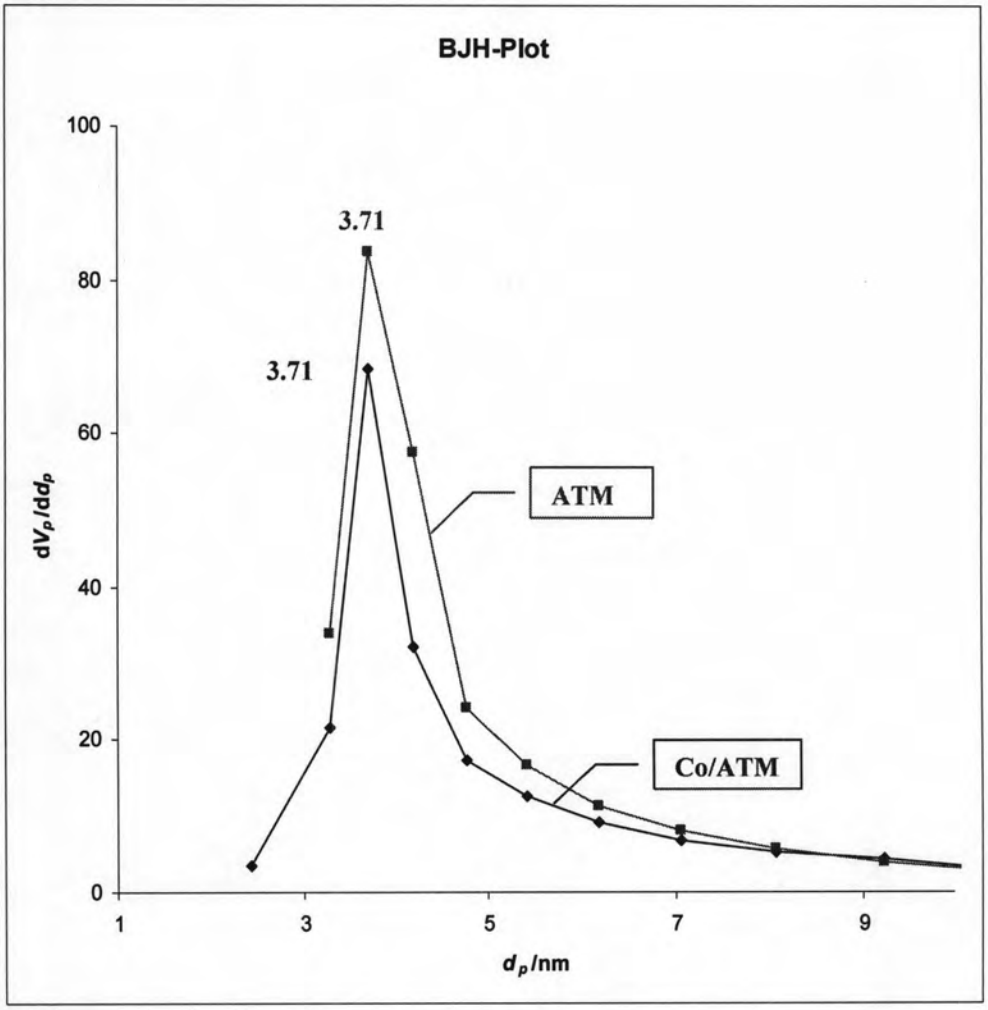

Figure 4.14 BJH pore size distributions of *in situ* generated MoS_2 and Co/MoS_2 catalysts from ATM.

The BJH pore size distributions of *in situ* generated MoS_2 catalyst from ATM precursor and Co/MoS_2 catalyst from ATM+Coacetate are presented in Figure 4.14. The MoS_2 and Co/MoS_2 catalysts from ATM precursor have narrow pore size distributions, ranging from 3 to 5 nm. Both of catalysts have the same pore size diameter of 3.71 nm., that pores are moderate pores.

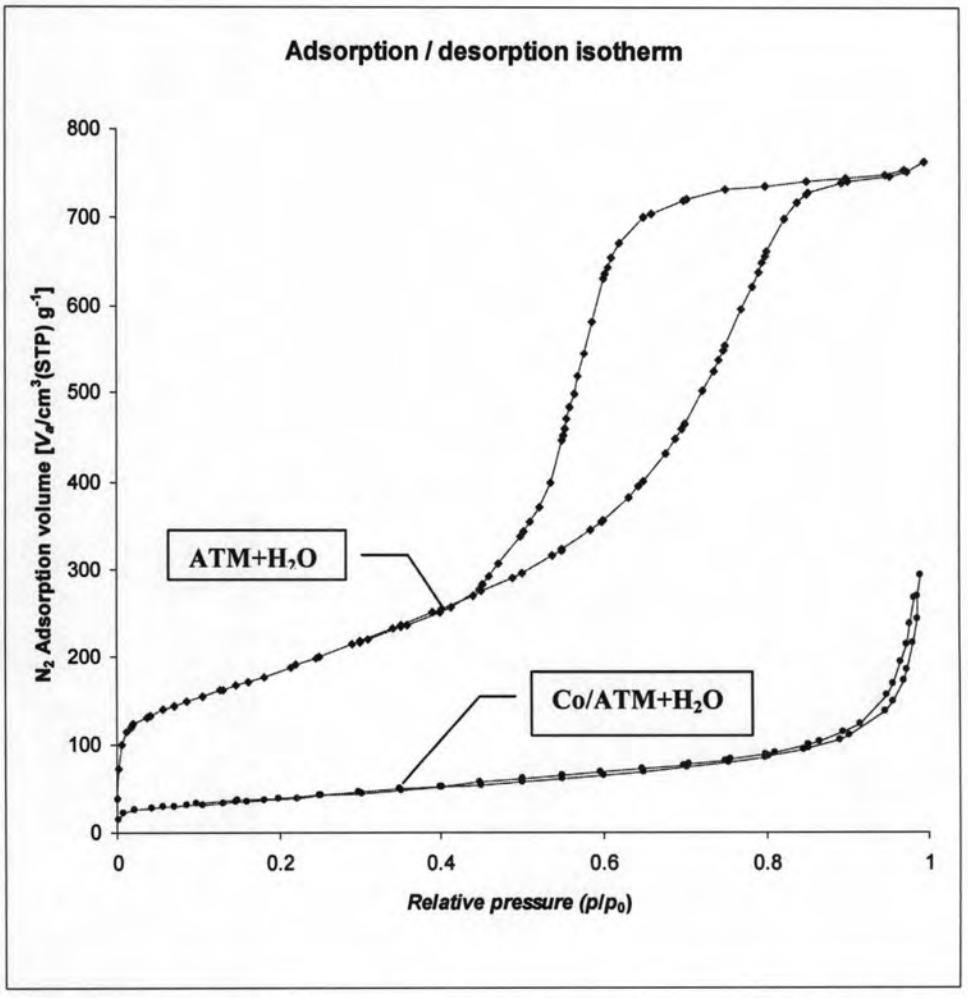

Figure 4.15 Adsorption-desorption isotherms for *in situ* generated MoS_2 and Co/MoS_2 catalysts from $ATM+H_2O$.

For the *in situ* generated MoS_2 catalyst from $ATM+H_2O$ presents only a type IV isotherms, type I isotherms can be considered for *in situ* generated Co/MoS_2 catalyst from $ATM+H_2O$+Coacetate.

The cobalt addition retards strongly the formation of an organized porous system. For instance, while a type IV isotherms is already formed for *in situ* generated MoS_2 catalyst from $ATM+H_2O$, only a poorly porous system is obtained for *in situ* generated Co/MoS_2 catalyst from $ATM+H_2O$+Coacetate with a type I isotherms and very low values of N_2 adsorption.

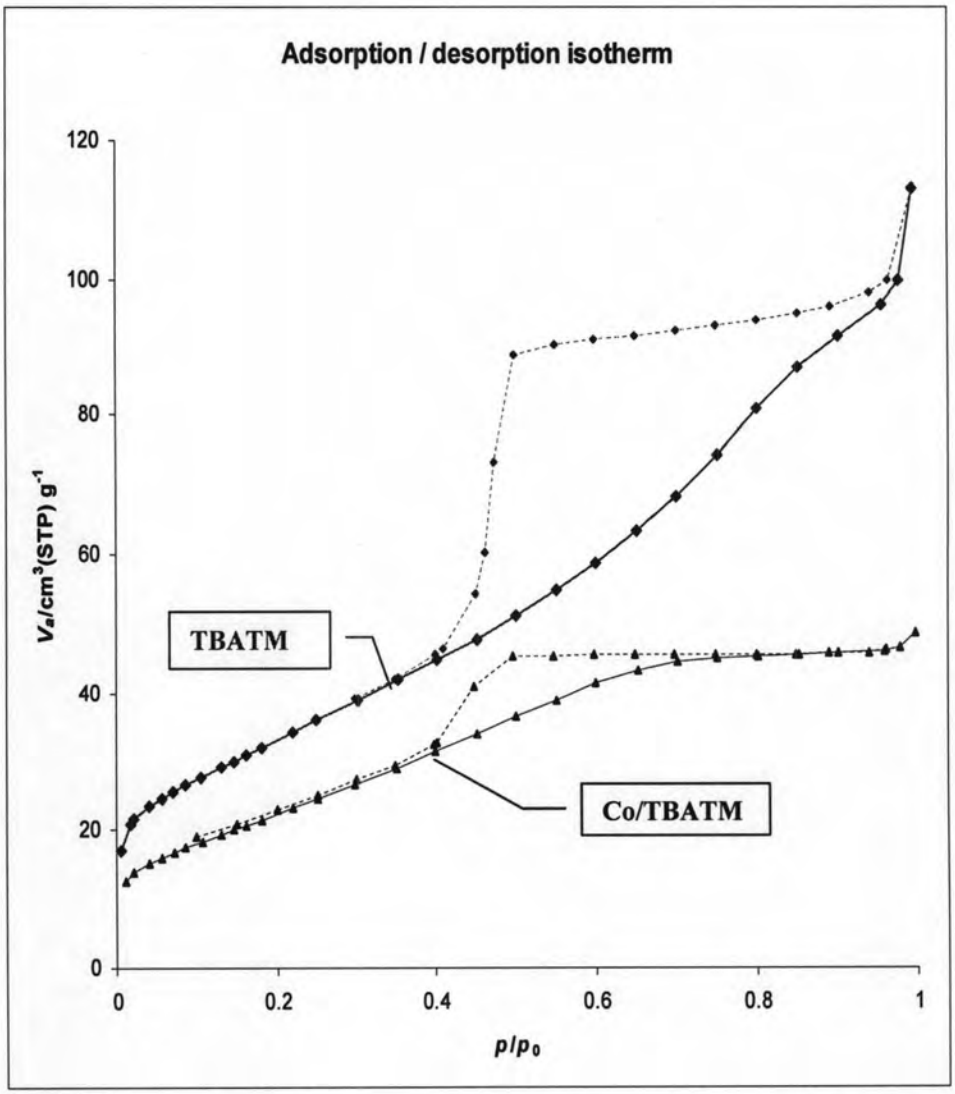

Figure 4.16 Adsorption-desorption isotherms for *in situ* generated MoS_2 and Co/MoS_2 catalysts from TBATM.

As shown in Figure 4.16, *in situ* generated Co/MoS_2 catalyst from TBATM shows a broad distribution of mesopores since the slope of the adsorption branch remains almost constant above P/P_0 = 0.4. The hysteresis loops shown by these catalysts correspond mainly to cylindrical pores open at both ends. However, some mesopores have narrow ends as in an ink-bottle pore shape, particularly for the *in situ* generated Co/MoS_2 from TBATM. The results are in good agreement with previous report [31].

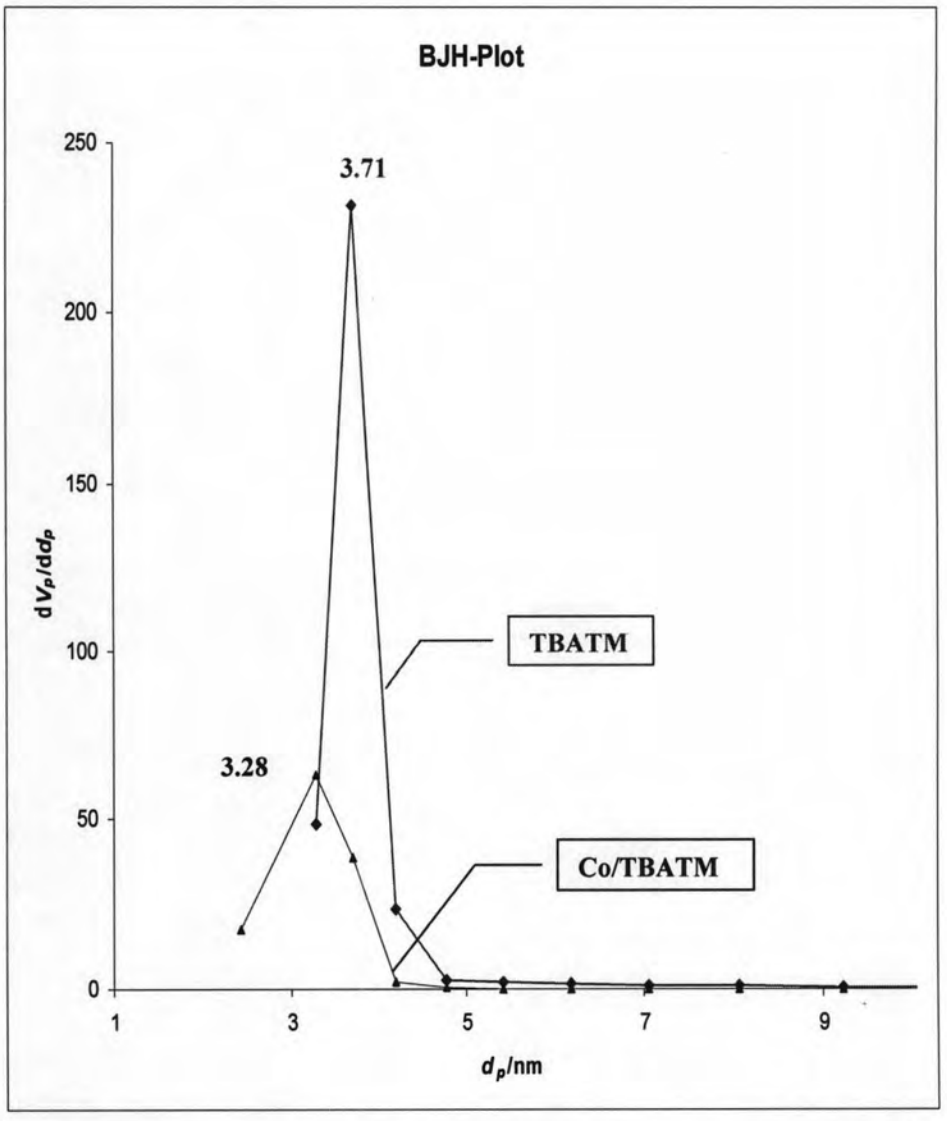

Figure 4.17 BJH pore size distributions of *in situ* generated MoS_2 and Co/MoS_2 catalysts from TBATM.

However, the hysteresis loop appears less developed and a narrower pore size distribution is obtained centered at a slightly larger pore diameter (3.71 nm) for *in situ* generated MoS_2 catalyst from TBATM precursor, while the *in situ* generated Co/MoS_2 catalysts from TBATM has pore diameter of 3.28 nm.

The hysteresis loops shown by these catalysts correspond mainly to cylindrical pores open at both ends. However, some mesopores have narrow ends as in an ink-bottle pore shape, particularly for the *in situ* generated Co/MoS_2 from TBATM [31].

4.3.4 Scanning electron microscope (SEM)

The SEM micrographs for *in situ* generated MoS_2 catalysts from ATM, ATM+H_2O, TBATM and TBATM+H_2O precursors were collected in Figures 4.18 and 4.19.

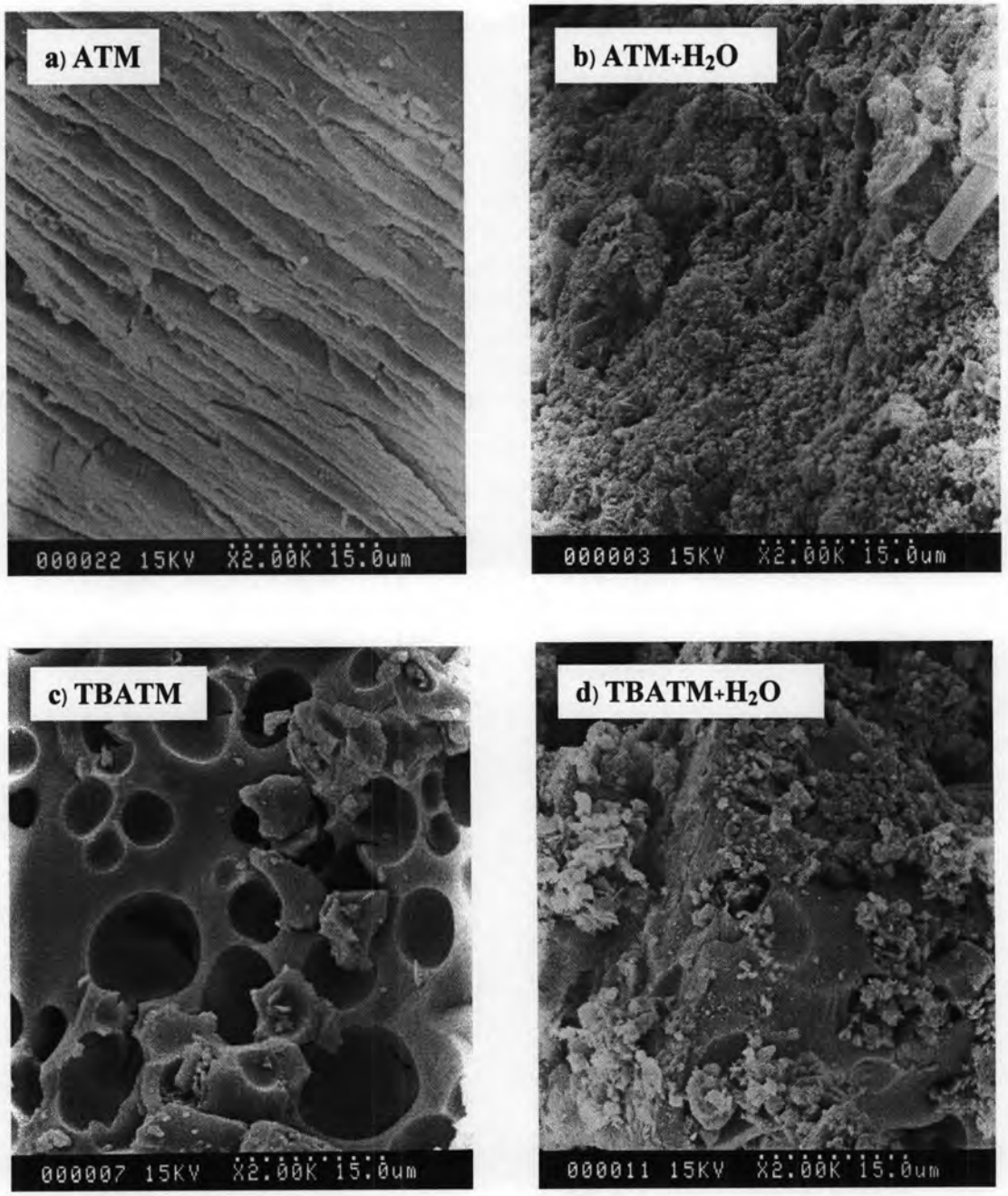

Figure 4.18 SEM micrographs of *in situ* generated MoS_2 catalysts (obtained *in situ* activation without substrate).

Figures 4.18 and 4.19 show SEM micrographs observed at a magnification of 2000x for the *in situ* generated MoS_2 catalysts. The SEM micrographs of *in situ* generated MoS_2 catalyst prepared by decomposition of ATM (Figure 4.18a) shows a flat and smooth surface with stack layer of MoS_2. On the other hand, *in situ* generated MoS_2 catalyst from ATM+H_2O (Figure 4.18b) reveals a highly porous and rough surface. This is in a good agreement with that reported [36].

The replacement of ATM by a tetrabutyllammonium precursor like TBATM involves a strong change in the morphology of *in situ* generated MoS_2 catalysts (Figures 4.18a and 4.18c). The *in situ* generated MoS_2 catalyst from TBATM has pronounced cheese-like cavities morphology with porous system. The "cheese" like morphology observed is produced by the internal pressure generated by the vaporization of the organic alkyl groups during the decomposition steps of TBATM precursor under high pressure of hydrogen and high temperature of the reaction media. Cavities are produced by the accumulation of gases during the decomposition [33].

Comparison between SEM micrographs of *in situ* generated MoS_2 catalysts from TBATM (Fig. 4.18c) and TBATM+H_2O (Fig. 4.18d), *in situ* generated MoS_2 from TBATM+H_2O still results in porous solid but cavities appear much smaller than TBATM. The water addition retards the formation of an organized porous system.

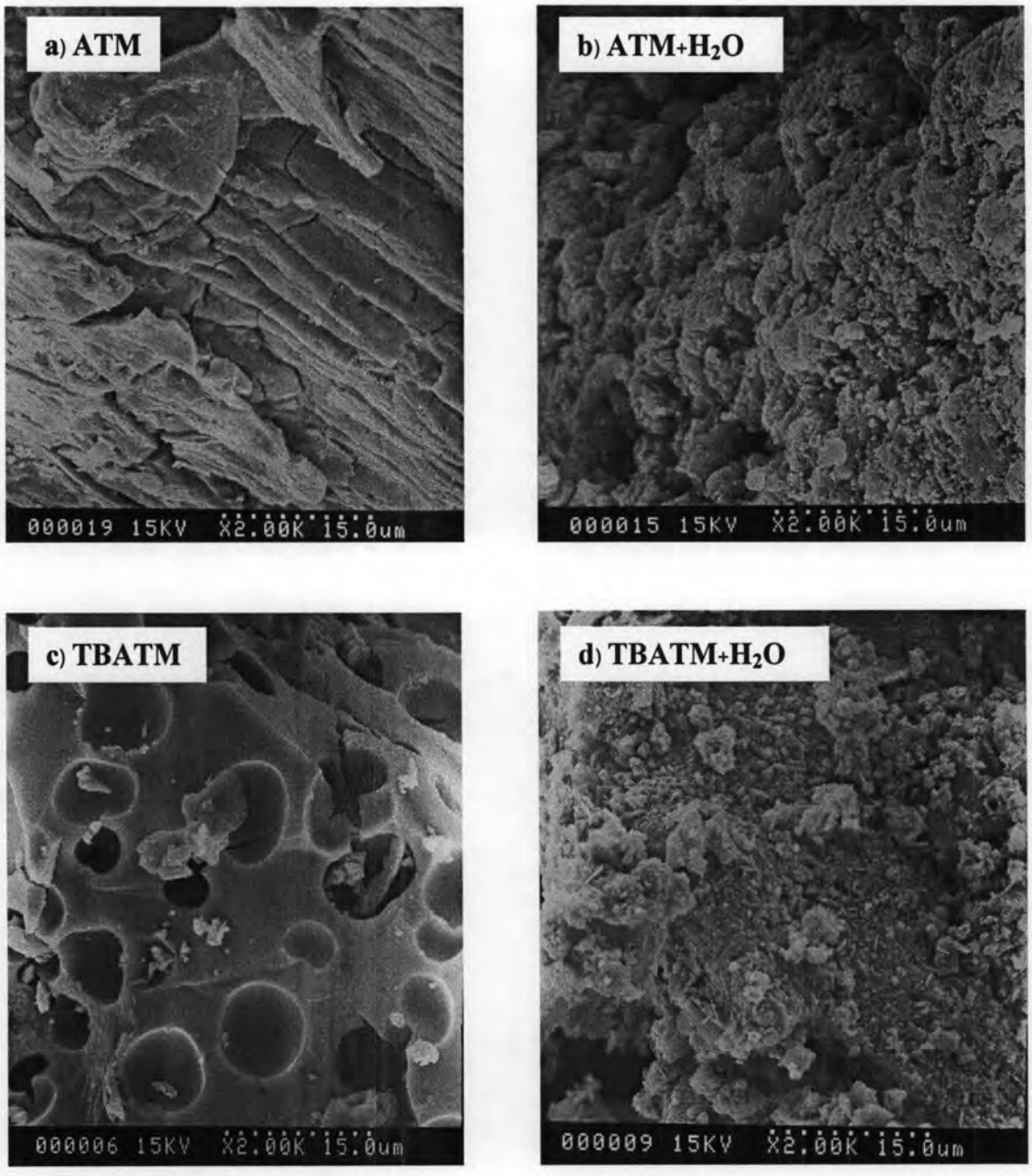

Figure 4.19 SEM micrographs of *in situ* generated MoS_2 catalysts (after HDS reaction).

Figure 4.19 shows SEM micrographs observed at a magnification of 2000x for *in situ* generated MoS_2 catalyst after HDS reaction. All these micrographs show similar features of MoS_2 obtained *in situ* activation without substrate (Figure 4.18).

For cobalt promoted ATM and TBATM precursors, SEM micrographs of *in situ* generated $CoMoS_2$ catalysts were shown in Figures 4.20 – 4.21.

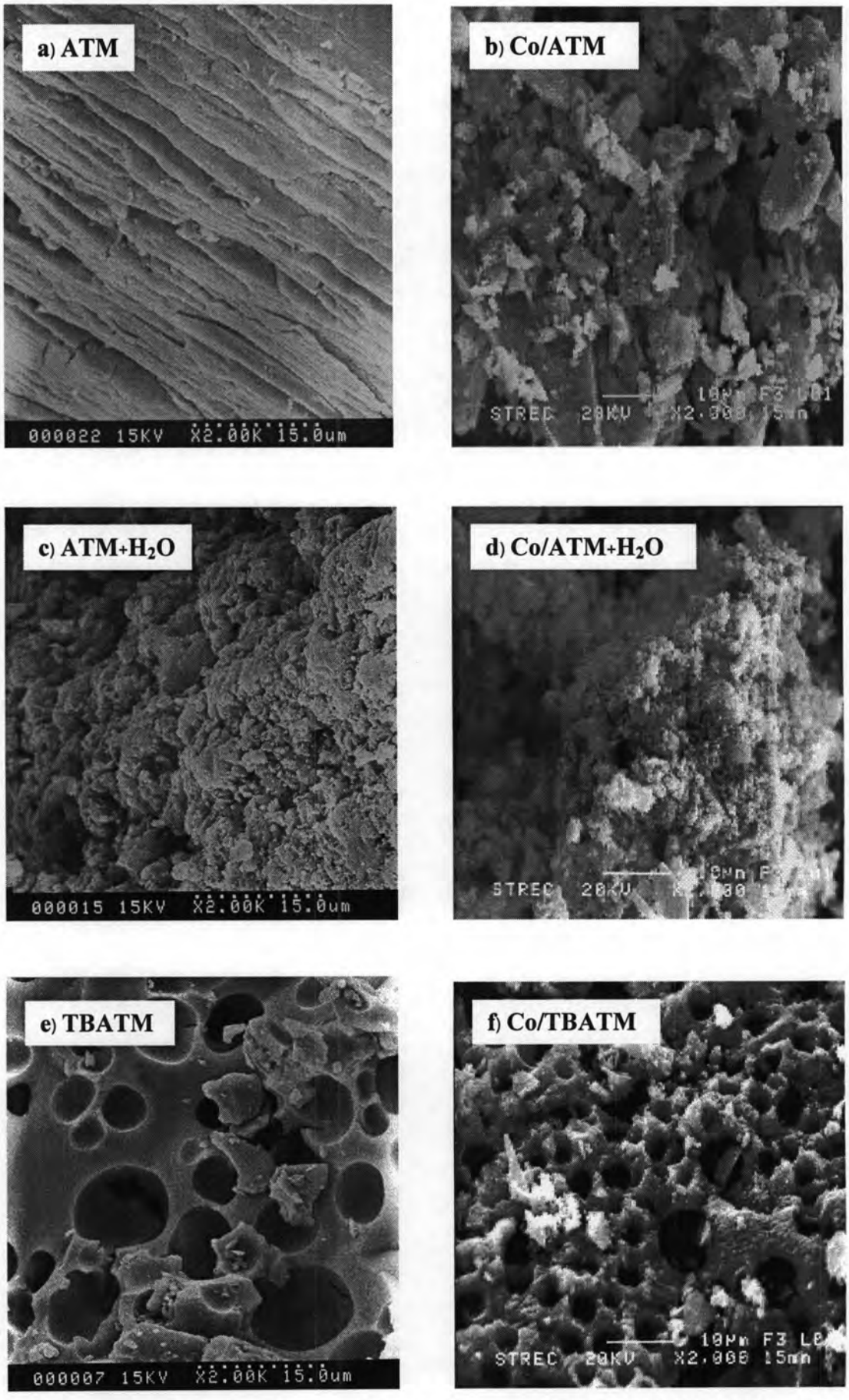

Figure 4.20 SEM micrographs of *in situ* generated MoS_2 and Co/MoS_2 catalysts (obtained *in situ* activation without substrate).

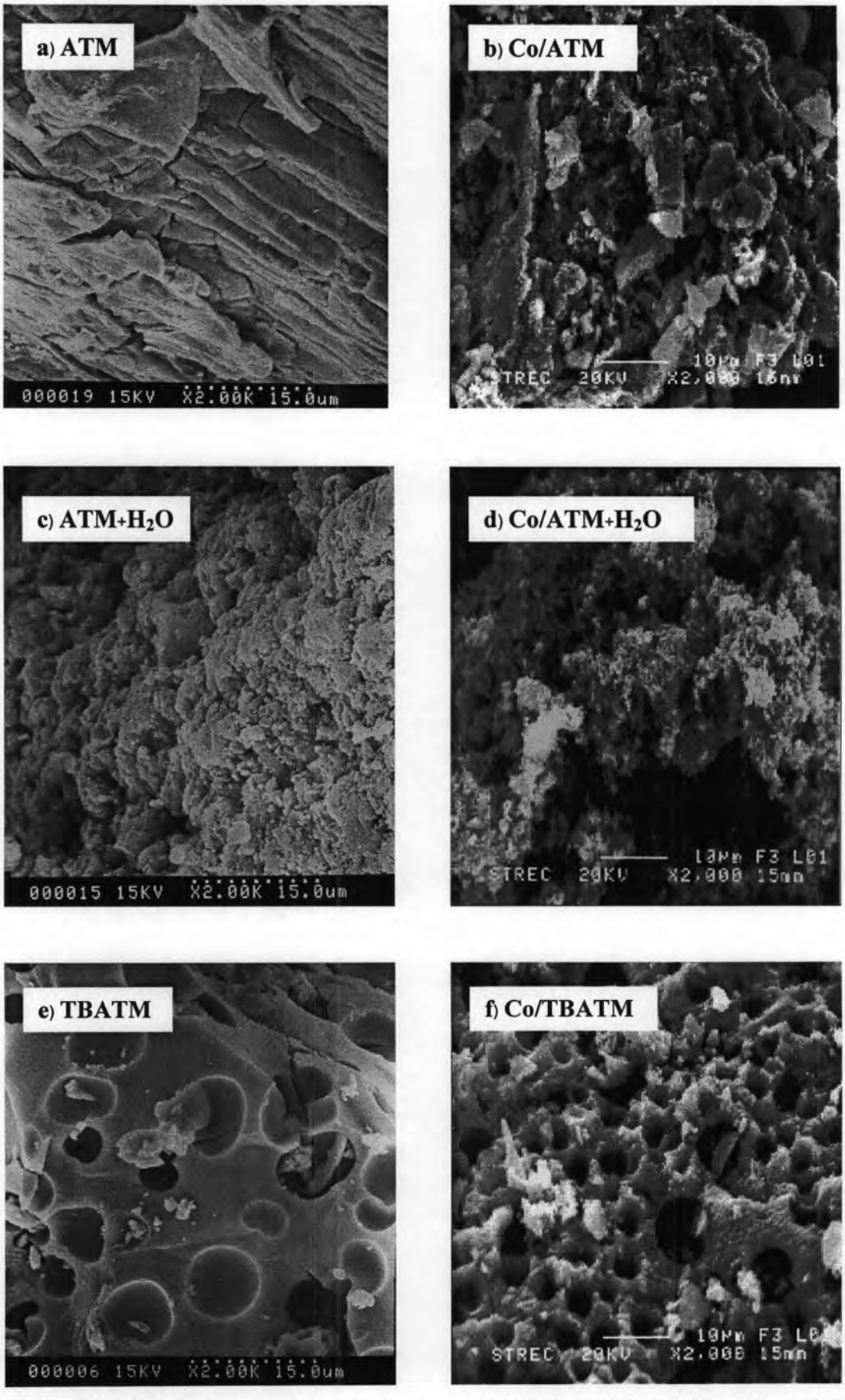

Figure 4.21 SEM micrographs of *in situ* generated MoS_2 and Co/MoS_2 catalysts (after HDS reaction).

The morphology of *in situ* generated Co/MoS_2 catalyst are shown in Figures 4.20b, d and f. The cobalt addition does not change markedly the morphology of the Co/MoS_2 catalysts compared with MoS_2 catalyst (Figures 4.20a, c and e).

Comparison between *in situ* generated MoS_2 catalysts from ATM (Fig. 4.20a) and *in situ* generated Co/MoS_2 catalyst from Co/ATM (Fig. 4.20b), the latter shows flat surface with agglomerated particles.

For *in situ* generated MoS_2 catalysts from ATM+H_2O (Fig. 4.20c) and *in situ* generated Co/MoS_2 catalyst from Co/ATM+H_2O (Fig. 4.20d), Co/MoS_2 catalyst still exhibited porous and rough surface but less than MoS_2 from ATM+H_2O.

Compared with SEM micrographs of *in situ* generated MoS_2 catalyst from TBATM (Fig. 4.20e) and *in situ* generated Co/MoS_2 catalyst from Co/TBATM (Fig. 4.20f), Co/MoS_2 catalyst present slightly smaller diameters of the cavities and wall between cavities appear thicker than MoS_2 catalyst.

4.4 Hydrodesulfurization of sulfur model compounds

4.4.1 Hydrodesulfurization of dibenzothiophene

Various factors were required to study the effect of the hydrodesulfurization of dibenzothiophene (DBT), a representative of sulfur model compounds. The parameters studied for hydrodesulfurization included reaction time, hydrogen pressure, catalyst precursor amount, types of catalyst precursor, effect of pyridine, effect of water addition and effect of promoters.

The hydrodesulfurization of dibenzothiophene yields two main products:

1. Biphenyl (BP) is resulted from direct desulfurization pathway (DDS).

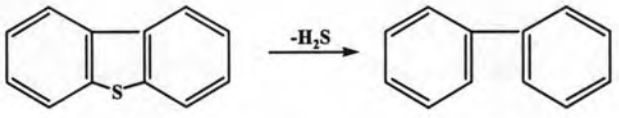

DBT BP (4.7)

2. Cyclohexylbenzene (CHB) through the hydrogenation pathway (HYD), obtained by C-S bond breaking followed by hydrogenation of one of aromatic rings of dibenzothiophene.

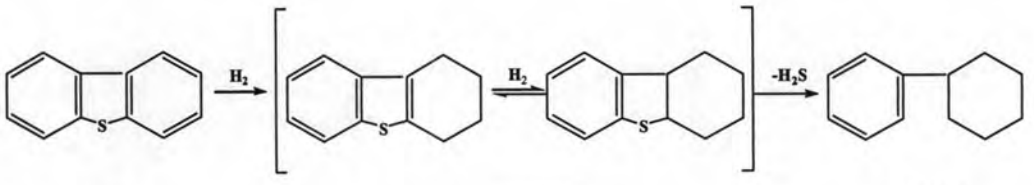

DBT THDBT CHB (4.8)

Since these two pathways are parallel [54], the ratio between HYD and DDS can be approximated in terms of the experimental selectivity by mean equation

$$HYD/DDS = (CHB)/(BP) \quad (4.9)$$

A. Effect of reaction time

Reaction time is one of the important parameters for hydrodesulfurization reaction. Hydrodesulfurization of dibenzothiophene was monitored with time, the results are pointed out in Table 4.2.

Table 4.2 Effect of reaction time on HDS of DBT

Entry	Reaction time (h)	%Conv. of DBT	Selectivity		HYD/DDS ratio
			%CHB	%BP	
1	0.5	45.9	9.1	19.5	0.5
2	1	68.8	11.5	23.1	0.5
3	1.5	88.1	20.5	38.9	0.5
4	2	99.6	28.4	49.8	0.6

Reaction conditions: DBT 0.368 g (2 mmol), ATM 0.052 g (0.2 mmol), decalin 50 mL 350 °C, 30 atmH_2.

As shown in Table 4.2, the increasing of the reaction time from 0.5 to 2 h. increased the HDS conversion of DBT. The highest conversion of DBT could be accomplished at 2 h. %conversion of DBT and %yield of products increased with the reaction time. It has been reported in many literatures [55], that the DBT conversion increases linearly with time as expected for pseudo-zero order reaction, indicating that rates remain constant during reaction.

B. Effect of hydrogen pressure

Hydrogen pressure is another important parameter for hydrodesulfurization condition. The hydrogen pressure was studied by varying hydrogen pressure from 20 to 30 atm, the results were shown in Table 4.3.

Table 4.3 Effect of hydrogen pressure on HDS of DBT

			Selectivity		HYD/DDS
Entry	**H_2 pressure (atm)**	**%Conv. of DBT**	**%CHB**	**%BP**	**ratio**
1	20	81.7	19.5	39.6	0.5
2	25	92.9	23.5	47.9	0.5
3	30	99.6	28.4	49.8	0.6

Reaction conditions: DBT 0.368 g (2 mmol), ATM 0.052 g (0.2 mmol), decalin 50 mL 350 °C, 2 h.

As shown in Table 4.3, when the reaction was carried out with 30 atm H_2 pressure, %conversion of DBT was evidently increased up to 99.6% (entry 3). It was explained that the increasing of hydrogen pressure enhances reaction of the reactants and the *in situ* generated MoS_2 catalyst. It has been reported that hydrogen can activate MoS_2 surfaces by reacting with surface sulfur to create vacancies on MoS_2 edge planes [56].

Another explanation might be that in the *in situ* decomposition, combination of low temperature of decomposition (350 °C) and high pressure of hydrogen (30 atm) can produce a very disordered MoS_2 structure with large surface area and improved catalytic activity. This can be due to the high hydrogen pressure which favors sulfur elimination through H_2S formation. It is known that amorphous MoS_3 (the first step of ATM decomposition) is very sensitive to the presence of H_2. During *in situ* activation in the presence of high pressure of hydrogen the composition of catalysts seems to be closer to MoS_2 [35].

C. Effect of catalyst precursor amount

Variable amounts of ammonium tetrathiomolybdate precursors were used to study for the hydrodesulfurization. The effect of catalyst precursor amount on the hydrodesulfurization of dibenzothiophene was shown in Table 4.4.

Table 4.4 Effect of catalyst precursor amount on HDS of DBT

Entry	mole ratio of DBT/Mo	%Conv. of DBT	Selectivity %CHB	Selectivity %BP	HYD/DDS ratio
1	10	68.8	11.5	23.1	0.5
2	20	42.1	5.4	18.9	0.3
3	50	32.4	2.9	15.9	0.2

Reaction conditions: DBT 0.368 g (2 mmol), ATM 0.052 g (0.2 mmol), decalin 50 mL 350 °C, 30 atm H_2, 1 h.

Table 4.4 shows the effect of varying the catalyst precursor amount. It was found that amount of catalyst precursor affected %conversion. When the amount of ATM was increased, %conversion of DBT was increased. The results showed that ATM precursor with 10 mole ratio of S/Mo gave the highest % conversion (68.8%).

The result is in good agreement with those report [57] for sulfided Mo/Al_2O_3 catalysts, increasing the Mo loading will increase the total HDS conversion, due to increase the total concentration of MoS_2 edge sites.

D. Effect of types of catalyst precursor

The effect of type of catalyst precursor on the hydrodesulfurization of dibenzothiophene was studied using two types of catalyst precursor and compared with MoS_2 commercial were observed in the same condition, the results are reported in Table 4.5.

Table 4.5 Effect of types of catalyst precursors on HDS of DBT

Entry	Catalyst precursor	%Conv. of DBT	Selectivity		HYD/DDS ratio
			%CHB	%BP	
1	MoS_2	13.5	1.1	7.1	0.2
2	ATM	68.8	11.5	23.1	0.5
3	TBATM	88.6	22.9	38.0	0.6

Reaction conditions: DBT 0.368 g (2 mmol), $MoS_2$0.032 g(0.2 mmol), ATM 0.052 g (0.2 mmol), TBATM 0.1416 g (0.2 mmol), decalin 50 mL, 350 °C, 30 atmH_2, 1 h.

From the comparative results of the HDS of DBT using different catalyst precursors in Table 4.5, MoS_2 gave only 13.5 %conversion of DBT. In the presence of ATM was used as a catalyst precursor, the conversion of DBT becomes significant, %conversion of DBT increased to 68.8%. For TBATM precursor, the highest conversion of DBT is 88.6%. The activity order of the catalyst precursor types in the HDS of DBT was TBATM > ATM > MoS_2.

The result is in good agreement with previous report [44], the *in situ* generated MoS_2 catalyst from decomposition of ATM is more active than that from sulfidation of molybdenum oxide or the reagent MoS_2.

Compared with the *in situ* generated MoS_2 catalyst from ATM and TBATM, the presence of butyl group in TBATM precursor has an important effect on the surface area and total pore volume of MoS_2 catalysts, leads to a strong increase in HDS activity. As shown by BET studies (section 4.3.2, Table 4.1) increasing in HDS activity might be due to *in situ* generated MoS_2 from TBATM with the high surface area is 270 m^2/g with the highest activities is 88.6% more active than MoS_2 formed from ATM precursor (120 m^2/g). These suggested that the catalytic activity depended on surface area of *in situ* generated MoS_2 catalyst.

E. Effect of pyridine

It is well known that nitrogen compounds inhibit the HDS reaction significantly. Pyridine was chosen as a model nitrogen compound. The effect of pyridine on the hydrodesulfurization of dibenzothiophene was investigated and the results were collected in Table 4.6.

Table 4.6 Effect of pyridine on HDS of DBT

Entry	Catalyst precursor	%Conv. of DBT	Selectivity		HYD/DDS ratio
			%CHB	%BP	
1	DBT	68.8	11.5	23.1	0.5
2	DBT + 10ppm pyridine	23.2	0.4	7.7	0.1
3	DBT + 40ppm pyridine	14.6	-	6.6	-
4	DBT + 70ppm pyridine	11.4	-	5.3	-

Reaction conditions: DBT 0.368 g (2 mmol), ATM 0.052 g (0.2 mmol), decalin 50 mL. 350 °C, 30 atmH_2, 1h.

From Table 4.6, it was observed that in the presence of pyridine, the results showed that pyridine severely inhibits the activity of the *in situ* generated MoS_2 catalyst for the HDS of DBT. The inhibition effect of pyridine is very strong, even at concentrations at low 10 ppm, %conversion of DBT was decreased from 68.8% (absence of pyridine, entry 1) to 23.2% (10 ppm pyridine, entry 2).

In the presence of pyridine (entries 2 – 4), It was found that pyridine affected product from HDS of DBT, biphenyl is the major product. When the concentration of pyridine in the reaction increased, %BP was decreased dramatically and CHB product not occured in the reaction (entries 3 and 4).

Similar results have been reported previously [58], over a sulfided $CoMo/Al_2O_3$ catalyst. Significant retardation on the hydrogenation (HYD) route of DBT and direct desulfurization (DDS) route was observed by the presence of nitrogen impurities, pyridine adsorbed competitively with the DBT on the active sites of

catalyst. However, the inhibition on the hydrogenation route is much more pronounced than direct desulfurization pathway.

F. Effect of water addition

It is well-known that water or steam deactivates hydrotreating catalysts, such as Mo-based catalyst, under conventional processing conditions [59]. Recently, it has been reported [44], for coal liquefaction using *in situ* generated MoS_2 catalyst from ammonium tetrathiomolybdate. It has been discovered that water addition have strong promoting effect on catalytic conversion of sub-bituminous coals.

In this work, the effect of water addition on the hydrodesulfurization of dibenzothiophene was also investigated. The results were collected as shown in Table 4.7.

Table 4.7 Effect of water addition on HDS of DBT

Entry	Catalyst precursor	mole ratio of H_2O/precursor	%Conv. of DBT	Selectivity %CHB	Selectivity %BP	HYD/DDS ratio
1	-	-	6.7	1.5	5.1	0.3
2	ATM	-	68.8	11.5	23.1	0.5
3	H_2O	450	-	-	-	-
4	ATM+H_2O	450	86.2	11.7	49.1	0.2
5	ATM+H_2O	600	91.9	12.9	52.4	0.2
6	TBATM	-	88.6	22.9	38.0	0.6
7	TBATM+H_2O	450	30.1	5.4	15.3	0.3
8	TBATM+H_2O	600	19.8	2.5	12.4	0.2

Reaction conditions: DBT 0.368 g (2 mmol), ATM 0.052 g (0.2 mmol), TBATM 0.1416 g (0.2 mmol), decalin 50 mL, 350°C, 30 atmH_2, 1h.

The results depicted in Table 4.7 demonstrated that without catalyst, the conversion of DBT was very low (entry 1). In the presence of the ATM precursor, the

DBT conversion is significant (entry 2). Water addition alone shows no promoting effect, instead, it inhibits the conversion of DBT (entry 3).

When added water to the runs with ATM (entry 4 – 5) substantially enhanced the catalytic reaction, % conversion of DBT increased from 68.8% (ATM alone; entry 2) to 86.2% at the molar ratio of H_2O/ATM = 450. In the similar reaction conditions, the conversion of DBT is the largest (91.9%) at the molar ratio of H_2O/ATM = 600, higher molar ratio of H_2O/ATM causes higher conversion of DBT.

These results reveal that using ATM and water together has a strong synergetic effect on DBT conversion. A beneficial effect of water addition to the catalytic reactions probably due to the change in the physical dispersion of catalyst precursor ATM in the presence of a suitable amount of water and organic solvent that would lead to production of the best catalyst under H_2 pressure [29]. It might be that ATM is dissolved in a suitable amount of H_2O which is dispersed (in fine droplets) in an organic solvent (under agitation) that decomposes upon heating under H_2 pressure to produce finely dispersed MoS_2 catalyst.

The extremely large surface area (BET) and small particle sizes (SEM) of the *in situ* generated MoS_2 catalyst from ATM+H_2O (section 4.3.2, Table 4.1) support the above considerations. The SEM micrographs of *in situ* generated MoS_2 catalyst from ATM shows a flat and smooth surface, while *in situ* generated MoS_2 catalyst from ATM+H_2O reveals a highly porous and rough surface. The high porosity of the surface of *in situ* generated MoS_2 catalyst from ATM+H_2O obtain to high surface area (544 m^2/g) than those from ATM alone (120 m^2/g).

As previous reported [29] that the solubility and dispersion effects of ATM and water are at work in hydrogenolysis of 4-(1-naphthylmethhyl)bibenzyl. ATM is soluble in water but insoluble in decalin solvent. The solubility of ATM in water is responsible, at least partly, for the generation of very fine and porous MoS_2-like particles from ATM with added H_2O in the presence of decalin solvent under H_2 pressure. In other words, the added water can dissolve ATM, and the presence of the organic solvent help to disperse the ATM-containing water droplet during agitation,

which give rise to the finely dispersed precursor molecules isolated by organic solvent prior to and during their decomposition and hydrogen reduction.

From the results in Table 4.7, the major product from HDS of DBT was biphenyl (BP), as widely reported [60]. It can be observed that the run with ATM+H_2O (entries 4 and 5), cyclohexylbenzene (CHB) product from HYD pathway was similar and biphenyl (BP) is the major product of HDS of DBT, % of BP product increased is about 2 times higher from 23.1% (ATM alone; entry 2) to 49.1% and 52.4% at the mole ratio of H_2O/ATM = 450 and 600 (entries 4 - 5). It is clear that the HDS pathways in ATM and ATM+H_2O runs are different.

In the case of TBATM, when TBATM+H_2O (entries 7 and 8) was added in the catalytic runs, an addition of water to the runs using TBATM shows lower %conversion of DBT in the both mole ratio of H_2O/TBATM, 30.1% and 19.8% at mole ratio of H_2O/TBATM at 450 and 600. From the results of surface area observed (section 4.3.2, Table 4.1), it was found that TBATM+H_2O have very less higher surface area (83 m^2/g) than those from TBATM alone (270 m^2/g), demonstrated that when added water to the runs of TBATM, % conversion of DBT decreased. That might be due to the decreasing of surface area of *in situ* generated MoS_2 catalyst from TBATM+H_2O caused the decreasing in the active sites of catalyst. This is also seen in SEM micrographs in this work(section 4.3.5), compared between SEM micrographs of TBATM (Figure 4.18c) and TBATM+H_2O (Figure 4.18d), cheese-like morphology with complicated porous system and cavity of *in situ* generated MoS_2 catalyst from TBATM+H_2O less than TBATM. It might be explained by morphology of *in situ* generated MoS_2, lower in porosity and cavities reduce the reactivity of active sites of *in situ* generated MoS_2 catalyst.

In the case of product selectivity for the TBATM precursor, when added water into the runs, it was found that the selectivity of products decreased in HYD/DDS ratio when added water to the runs from 0.6 (TBATM, entry 6) to 0.3 and 0.2 for TBATM+H_2O at mole ratio of H_2O/TBATM = 450 and 600. The possible explanation may be because that either an increase of active sites for the hydrogenolysis of DBT or a decrease of hydrogenation sites occurs.

G. Effect of cobalt or nickel promoter

Based on preliminary studies in section 4.4.1F, it was found that *in situ* generated MoS_2 catalyst from TBATM+H_2O shows lower HDS conversion of DBT. For this section, the approaches to improve performance in HDS activity of *in situ* generated MoS_2 catalyst was investigated.

It is widely well-known [61] that addition of a first-row transition element, most commonly cobalt and nickel compounds generally enhanced the HDS activity of catalysts at Co/Mo molar ratio of approximately 0.3. Therefore in this work, cobalt and nickel compounds at metal/Mo molar ratio of 0.3 were added in the reaction to study the effect of promoters on the HDS of DBT.

In this work, the effect of different cobalt compounds: cobalt(II) acetate ($Co(CH_3COO)_2$), cobalt(II) acetylacetonate ($Co(C_5H_7O_2)_2$), cobalt(II) chloride ($CoCl_2$), cobalt(II) nitrate ($Co(NO_3)_2$), cobalt oxide (CoO) and nickel compounds: nickel(II) acetylacetonate ($Ni(C_5H_7O_2)_2$) and nickel(II) nitrate ($Ni(NO_3)_2$) used as promoters for HDS of DBT were investigated and the results are collected in Table 4.8.

Table 4.8 Effect of TBATM precursor with cobalt or nickel promoters addition on HDS of DBT

Entry	Precursor	Promoter	%Conv. of DBT	Selectivity %CHB	Selectivity %BP	HYD/DDS ratio
1	TBATM	-	63.5	5.7	27.7	0.2
2	TBATM	$CoCl_2$	66.4	5.2	21.5	0.2
3	TBATM	$Co(C_5H_7O_2)_2$	73.4	12.2	32.3	0.4
4	TBATM	$Co(NO_3)_2$	78.8	7.0	28.0	0.2
5	TBATM	CoO	80.7	9.8	27.3	0.3
6	TBATM	$Co(CH_3COO)_2$	85.1	9.9	31.3	0.3
7	TBATM	$Ni(C_5H_7O_2)_2$	70.6	6.8	21.7	0.3
8	TBATM	$Ni(NO_3)_2$	73.7	9.2	23.5	0.4
9	-	$Co(CH_3COO)_2$	16.7	0.7	4.1	0.2

Reaction conditions: DBT 0.368 g (2 mmol), TBATM 0.071 g (0.1 mmol), decalin 50 mL, 350 °C, 30 atmH_2, 1 h.

From the results in Table 4.8, it was revealed that in the addition of a small amount of cobalt or nickel promoters enhanced HDS activity, the conversion of DBT was increased. The promoter effect has been attributed to the amount of Co or Ni atoms that can be accommodated on the edges of MoS_2 layers, and also to the electronic transfer that Co or Ni atoms induces on Mo atoms [62].

Compared with cobalt and nickel promoters, cobalt addition shows higher HDS activity than nickel addition. Similar results have been reported in the literature [63], that Co/MoS_2 catalyst usually shows higher activity than Ni/MoS_2 catalyst for HDS of DBT.

In the reaction carried out with TBATM precursors, the effect of promoters and the order of the promoter activities are as follows:

$$Co(CH_3COO)_2 > CoO \sim Co(NO_3)_2 > Co(C_5H_7O_2)_2 > CoCl_2$$

It has been reported in the literature [64] studied the influence of organic and nitrate precursors on the particle size of alumina-supported cobalt catalysts. The use of acetate and acetyl acetonate as cobalt precursors result in a higher activity compared with catalyst prepared from cobalt nitrate. The activities determined can be slightly correlated with an increasing cobalt dispersion, organic precursors were found to result in the formation of small particles. While, nitrate precursors formed larger particles.

Similar results were obtained when different cobalt precursors (nitrate, chloride, acetate and acetylacetonate) were supported on silica SBA-15 and MCM-14 [65, 66]. The use of cobalt acetate resulted in a number of small cobalt particles dispersed throughout MCM-41 and some larger particles located on the external surface of MCM-41.

Indeed, cobalt chloride exhibited lower activity due to poisoning by chloride ions [67]. The use of cobalt chloride resulted in very large cobalt particles/clusters and/or residual Cl^--blocking active sites, and, consequently, very small active surface area was measurable.

Effect of cobalt addition was also investigated for HDS of DBT catalyzed by *in situ* generated MoS_2 catalyst from ATM precursor with and without added water. The results summarized in Table 4.9.

Table 4.9 Effect of ATM precursor with cobalt promoters addition on HDS of DBT

Entry	Precursor	Promoter	%Conv. of DBT	Selectivity		HYD/DDS ratio
				%CHB	%BP	
1	-	$Co(CH_3COO)_2$	16.7	0.7	4.1	0.2
2	ATM	-	42.1	5.4	18.9	0.3
3	ATM	$Co(CH_3COO)_2$	73.9	5.8	15.5	0.4
4	ATM+H_2O	-	66.4	5.2	21.5	0.2
5	ATM+H_2O	$Co(CH_3COO)_2$	94.3	13.4	34.5	0.4

Reaction conditions: DBT 0.368 g (2 mmol), ATM 0.026 g (0.1 mmol), decalin 50 mL, 350°C, 30 atmH_2, 1 h.

As shown in Table 4.9, when used ATM as precursor (entry 2 – 5), HDS activity also increased when promoted with cobalt compound. For comparison, when cobalt acetate was tested separately, HDS conversion of DBT was 16.7% (entry 1).

When used ATM promoted with Co(acetate) (entry 2 – 3), HDS activity also increased from 42.1% (ATM non-promoted, entry 2) to 73.9% (ATM promoted with Co(acetate), entry 3). In the case of *in situ* generated Co/MoS_2 from ATM+H_2O, addition of Co(acetate) also enhanced HDS conversion from 66.4% (ATM+H_2O, entry 4) to 94.3% (ATM+H_2O promoted with Co(acetate), entry 5).

From the results, it can be observed that the run with ATM+H_2O promoted with Co(acetate) show the highest activity. It might be due the presence of water help to disperse the ATM precursor and cobalt promoter that would lead to production of the best catalyst under H_2 pressure. From the results of XRD analysis observed (section 4.3.1 figure 4.7), XRD pattern of *in situ* generated Co/MoS_2 catalysts from ATM+H_2O present very weak in intensity of peaks of Co phases, suggesting that cobalt atoms are well dispersed on the active phase.

4.4.2 Hydrodesulfurization of 4,6-dimethyldibenzothiophene

Since there appears to be a major effect of water on the catalytic reactions, the molar ratio of H_2O/ATM was attempted to determine the optimum amount of added water for the generation *in situ* MoS_2 catalyst, by examining the relationship between conversion of HDS reaction and amount of added water.

The hydrodesulfurization of 4,6-dimethyldibenzothiophene yields two main products:

1. Dimethybiphenyl (DMBP) through the so-called direct desulfurization pathway (DDS).

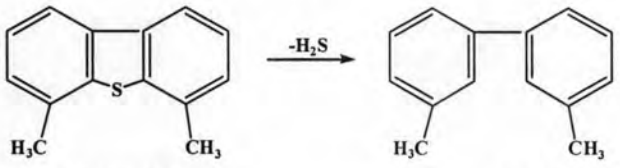

4,6-DMDBT **DMBP** (4.10)

2. Methylcyclohexyltoluene (MCHT) through the hydrogenative pathway (HYD).

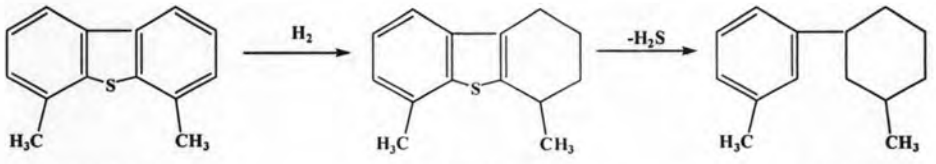

4,6-DMDBT **THDMDBT** **MCHT** (4.11)

Methylcyclohexyltoluene is a secondary product along this pathway obtained by C-S bond breaking reaction from tetrahydrodimethyldibenzothiophene (THDMDBT), an intermediate product formed by hydrogenation of one of aromatic rings of 4,6-dimethyldibenzothiophene [68].

Since these two pathways are parallel [68], the ratio between HYD and DDS can be approximated in terms of the experimental selectivity by mean equation

$$HYD/DDS = (MCHT)/(DMBP) \quad (4.12)$$

The results of the addition of water studied and optimum range of the ratio of H_2O to ATM in HDS reaction of 4,6-DMDBT are collected in Table 4.10.

Table 4.10 Effect of water addition and specific surface area of *in situ* generated MoS_2 catalyst on HDS of 4,6-DMDBT

Entry	Catalyst precursor	mole ratio of H_2O/ATM	%Conv. of 4,6-DMDBT	Selectivity		HYD/DDS ratio
				%MCHT	%DMBP	
1	ATM	-	47.2	5.1	9.3	0.5
2	ATM+H_2O	750	93.0	8.7	24.3	0.4
3	ATM+H_2O	900	93.5	7.2	25.7	0.3
4	ATM+H_2O	1200	100.0	6.2	26.4	0.2
5	ATM+H_2O	2000	93.7	5.9	32.7	0.2

Reaction conditions: 4,6-DMDBT 0.212g (1 mmol), ATM 0.026 g (0.1 mmol), decalin 50 mL, 350 °C, 30 atmH_2, 2 h.

Table 4.10 summarized the catalytic activities of *in situ* generated MoS_2 catalysts from ATM with added water. The major product from 4,6-DMDBT was dimethylbiphenyl (DMBP) through direct desulfurization. Methylcyclohexyltoluene (MCHT) was the minor product as observed in this work.

The results demonstrated that in the presence of ATM without added water, the conversion of 4,6-DMDBT is 47.2% (entry 1).

When added water to the runs with ATM (entries 2 – 5), the addition of water significantly increased the HDS activities. The conversion of 4,6-DMDBT increased, 93.0% and 93.5%, respectively at the mole ratio of H_2O/ATM about 750 and 900.

The HDS conversions of 4,6-DMDBT gradually increase from 47.2% to 100.0% with increasing water amount from 0 to 2.16 ml (entry 5) corresponding to a mole ratio of H_2O/ATM around 1200, and they decrease from 100.0% to 93.7% (entry 6) with further addition of water at mole ratio of H_2O/ATM around 2000. From the results, it appears that too much of water may overthrow the balance of aqueous phase-organic phase. Furthermore, a large excess amount of water seems to make the negative effect of added water on HDS of 4,6-DMDBT, suggests that water itself may

have an inhibiting effect on the HDS of 4,6-DMDBT. Probably water can also compete with reactant 4,6-DMDBT molecules through competitive chemisorption on surface sites of the *in situ* generated MoS_2 catalyst and thus can inhibit the HDS conversion of 4,6-DMDBT.

The similar result is observed with previous report [69] on hydrodesulfurization of diesel using ATM precursor when added water 21 mL in the 50 mL of diesel , sulfur removal decreased from 90.5% to 59.8%, excess of water addition hinder the creation of the active sulfided species or facilitate their reoxidation.

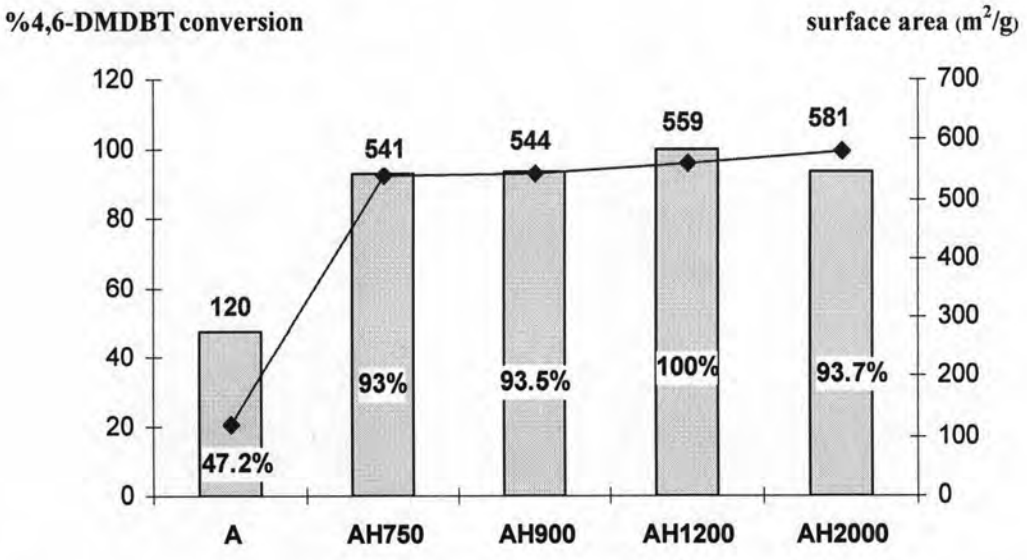

Figure 4.22 Specific surface area of *in situ* generated MoS_2 catalysts from ATM+H_2O and %conversion of 4,6-DMDBT.

Compared specific surface area of *in situ* generated MoS_2 catalyst with %conversion of 4,6-DMDBT, increasing of specific surface area, increased %conversion of 4,6-DMDBT at every mole ratio of H_2O/ATM exclude in the mole ratio of H_2O/ATM at 2000. At this ratio, added water can generated very high surface area of MoS_2 (581m^2/g) but droped in %conversion of 4,6-DMDBT to 93.70%. This might be due to further increasing water addition, decreased the HDS conversion of 4,6-DMDBT. It suggests that water itself may have an inhibiting effect on the HDS of 4,6-DMDBT.

4.5 Hydrodesulfurization of real oil feedstocks

In order to investigate whether the HDS system is effective for real oil feedstock, the HDS of straight run gas oil (6100 ppmS) and light cycle oil (310 ppmS) were carried out at 350 °C at 30 atm H_2 pressure. The desulfurized oil samples were analyzed in terms of total sulfur content using X-ray fluorescence (XRF; method ASTM D2622 (1994)).

The conversions of the individual sulfur components in SRGO analyzed by gas chromatography using a flame ionization detector (GC-FID) and each components were identified by comparing its retention time with that of standard compounds, the retention time are 3.281min for thiophene (T), 6.061 min for benzothiophene (BT), 10.420 min for dibenzothiophene (DBT) and 11.461 for 4,6-dimethyldibenzo-thiophene (4,6-DMDBT). By calculating the peak areas, each sulfur compound can be quantified.

4.5.1 Hydrodesulfurization of straight run gas oil (SRGO)

Hydrodesulfurization of straight run gas oil (SRGO) with 6100 ppmS. (9.531 mmolS) was performed at 350 °C, 30 atm H_2 pressure for 2 h., using *in situ* generated MoS_2 catalyst from ATM precursor with added water.

The results of hydrodesulfurization of SRGO catalyzed by *in situ* generated MoS_2 catalysts from ATM with added water are presented in Figure 4.22 and the conversions of the individual components is depicted as shown in Figure 4.23

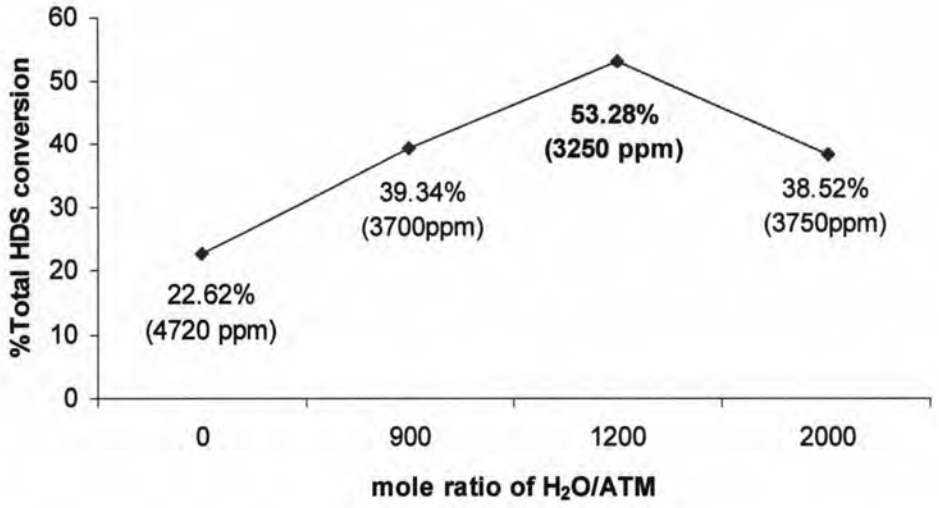

Figure 4.23 Total HDS conversions of straight run gas oil (SRGO) catalyzed by *in situ* generated MoS_2 catalyst from ATM with added water.

As shown in Figure 4.23, the total HDS conversion of straight run gas oil (SRGO) as feedstocks. The results indicated that all added water show favorable effects, total sulfur greatly reduce. Adding water with H_2O/ATM molar ratio = 900 (39.3 %conversion) enhanced HDS conversion to as much as H_2O/ATM molar ratio = 2000 (38.5 %conversion) while without added water showed 22.6 %conversion. Adding water with H_2O/ATM molar ratio = 1200 greatly accelerated HDS to achieve 53.2 %conversion. The total sulfur content was reduced from 6100 ppm (untreated SRGO) to 4720 ppm (treated with ATM alone) and to 3250 ppm (treated with ATM+H_2O at molar ratio of H_2O/ATM = 1200).

The results obtained when using *in situ* generated MoS_2 catalyst from ATM with added water to catalyzed SRGO as feedstock were similar from those obtained in the 4,6-DMDBT HDS model reaction (section 4.2, Table 4.10).

The conversion of the individual sulfur components (GC-FID method) in SRGO after HDS reaction also depicted in Figure 4.24.

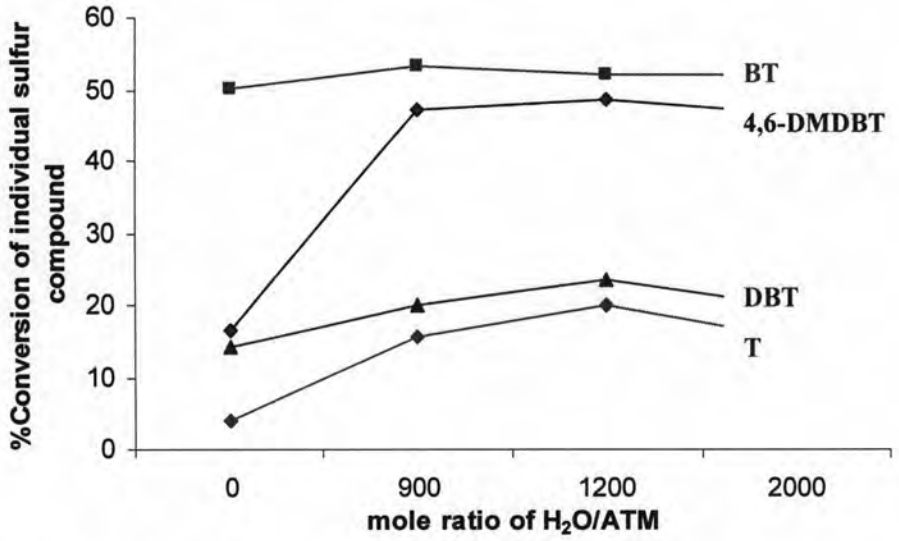

Figure 4.24 %Conversion of individual sulfur compounds in SRGO catalyzed by *in situ* generated MoS_2 catalyst from ATM with added water.

Figure 4.24 shows %conversion of four individual sulfur compounds, T, BT, DBT and 4,6-DMDBT in SRGO. The reactivities of each sulfur compounds can be ordered as follow:

BT > 4,6-DMDBT > DBT > T

It has been reported in most of literature [70], the reactivity order of sulfur compounds decreased in the order:

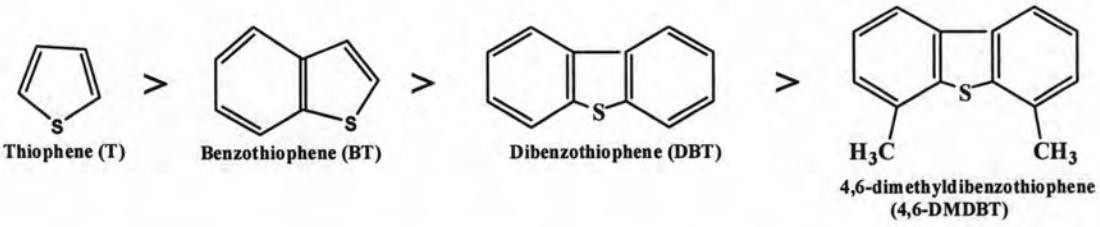

It seemed that HDS reactivity depends on the molecular size and structure of the sulfur-containing compound. Indeed, the approach of the sulfur atom to the active sites is particularly obstructed then substituents are in positions 4- and 6- in DBTs, making 4,6-DMDBT compounds particularly refractory to the HDS processes [71].

However, there are some discrepancies of reactivities of sulfur compounds in the literature. For the reaction of T and BT catalyzed by Co-Mo/Al_2O_3 at 300 °C, 71 atm H_2 pressure, it was found that reactivities of T < BT [72]. For the reaction of BT and DBT catalyzed by sulfided CoO-MoO_3/Al_2O_3 at 350 °C for 10 h., it was found that reactivities of BT > DBT [73, 74]. The result suggested that the reactivities of these compounds change depending on the reaction conditions and that it is difficult to compare the results obtained under different conditions.

It has been in previous report [16], the HDS of middle distillates catalyzed by Ni-Mo/Al_2O_3 catalyst at 340 °C, 50 atm H_2 for 3 h. The reactivity order of sulfur compounds decreased in the order: 4,6-DMDBT > DBT > 4-MDBT .

In the literature [75], suggested a very strong inhibiting matrix effect of components in the gas oil could be a part of the explanation of the observed inconsistencies in the relative reactivity found in the literature. Moreover, in the real oil feedstocks contains various components such as aromatics and N-containing hydrocarbons, the effect of components on catalytic activity become large under HDS conditions.

Table 4.11 Straight run gas oil (SRGO) properties

Properties	Straight run gas oil
Total sulfur (ppm)	6100
Total nitrogen (ppm)	68
Aromatic (%wt)	
mono-aromatic	24.95
diaromatic	3.82
polyaromatic	0.39

The properties of straight run gas oil (SRGO) in present work were shown in Table 4.11, consist of various components which include saturated and aromatic hydrocarbons, sulfur compounds and nitrogen compounds.

In this work, the reactivities of sulfur compounds, T, BT, DBT and 4,6-DMDBT in decalin solvent was investigated to examine inhibiting matrix effect in SRGO. In order to investigate the inhibiting matrix effect of various components affected the differences in the reactivities of individual sulfur species between real oil feedstocks; SRGO and the model reaction using synthesized thiophene (T), benzothiophene (BT), dibenzothiophene (DBT) and 4,6-dimethylbenzothiophene (4,6-DMDBT) were separately studied in decalin solvent under the same conditions as those of SRGO. The initial sulfur concentration of T, BT, DBT and 4,6-DMDBT in a model reaction using decalin was about 0.15 mmol is based on the concentration of sulfur species in SRGO, while that of T, BT, DBT and 4,6-DMDBT in SRGO is 0.004, 0.03, 0.13 and 0.18 mmol, respectively.

Hydrodesulfurization of T, BT, DBT and 4,6-DMDBT in decalin solvent carried out in the same condition of HDS of SRGO at 350°C at 30 atm H_2 pressure. The reactivities of each sulfur compounds, T, BT, DBT and 4,6-DMDBT in decalin solvent were presented in Figure 4.25.

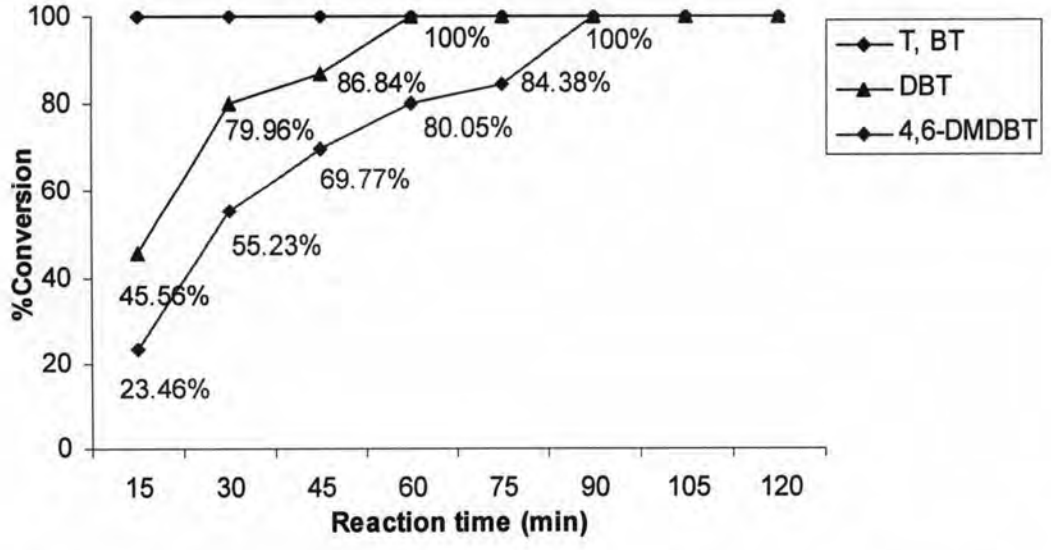

Figure 4.25 %Conversion of thiophene (T), benzothiophene (BT), dibenzothiophene (DBT) and 4,6-dimethyldibenzothiophene (4,6-DMDBT) in decalin solvent.

Figure 4.25 clearly shows that thiophene (T) and benzothiophene (BT) were completely converted 100% in 15 minutes. However, the conversions of both DBT and 4,6-DMDBT were 45.6 % and 23.5 %, respectively. DBT and 4,6-DMDBT were converted to 100.0% in 60 and 90 minutes, respectively. From the result in model solvent, it was showed that the reactivity decreased in the order:

T > BT > DBT > 4,6-DMDBT

When compared result of order reactivities of sulfur species; T, BT, DBT and 4,6-DMDBT in decalin solvent (Figure 4.25) with the result in SRGO (Figure 4.24):

SRGO : BT > 4,6-DMDBT > DBT > T
Decalin solvent : T > BT > DBT > 4,6-DMDBT

From the result mentioned above provided evidence confirming the reactivity of individual sulfur compounds in model solvent. The decreasing order of T, BT, DBT, and 4,6-DMDBT in decalin solvent was followed as a theory. It was confirmed that the deviation of reactivity of these sulfur compounds resulted from the effect of various components such as aromatics and N-containing hydrocarbons in SRGO. This clearly shows the extent of retarding effects of components in SRGO.

4.5.2 Hydrodesulfurization of light cycle oil (LCO)

Hydrodesulfurization of light cycle oil (LCO) performed in the same condition of HDS of SRGO at 350 °C at 30 atm H_2 pressure. The results of HDS of LCO catalyzed by *in situ* generated MoS_2 catalysts from ATM with added water are presented in Figure 4.26.

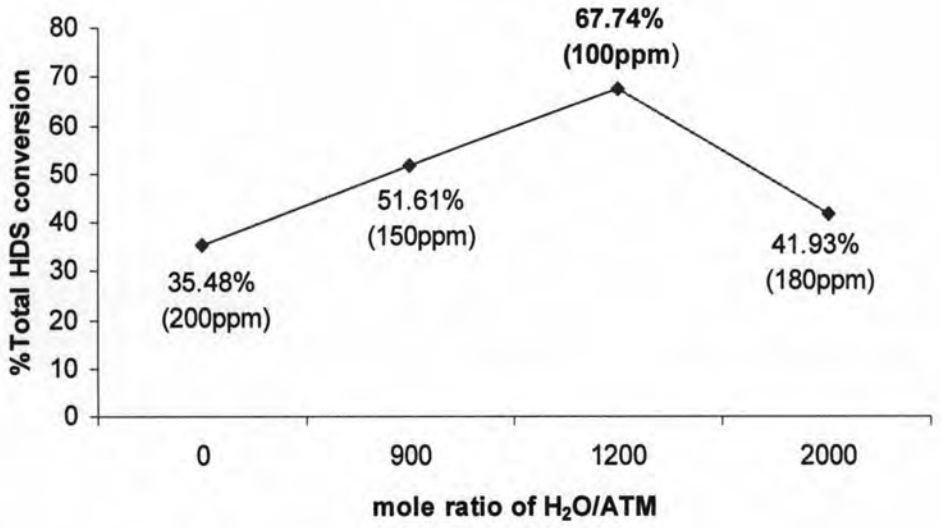

Figure 4.26 Total HDS conversions of light cycle oil (LCO) catalyzed by *in situ* generated MoS_2 catalyst from ATM with added water.

Figure 4.26 depicts the total HDS conversion of LCO as feedstocks. All added water show favorable effects, total sulfur greatly reduce. The HDS activity increased sharply with increasing H_2O/ATM molar ratio.

Adding water with H_2O/ATM molar ratio = 900 (51.6 %conversion) enhanced HDS conversion to as much as H_2O/ATM molar ratio = 2000 (41.9 %conversion) while without added water showed 35.5 %conversion. Adding water with H_2O/ATM molar ratio = 1200 greatly accelerated HDS to achieve 67.7 %conversion. The total sulfur content was reduced from 310 ppm (untreated LCO) to 200 ppm (treated with ATM alone) and to 100 ppm (treated with ATM+H_2O at molar ratio of H_2O/ATM = 1200).

The conversion of the individual sulfur components (GC-FID method) in light cycle oil (LCO) after HDS reaction also shown in Figure 4.27.

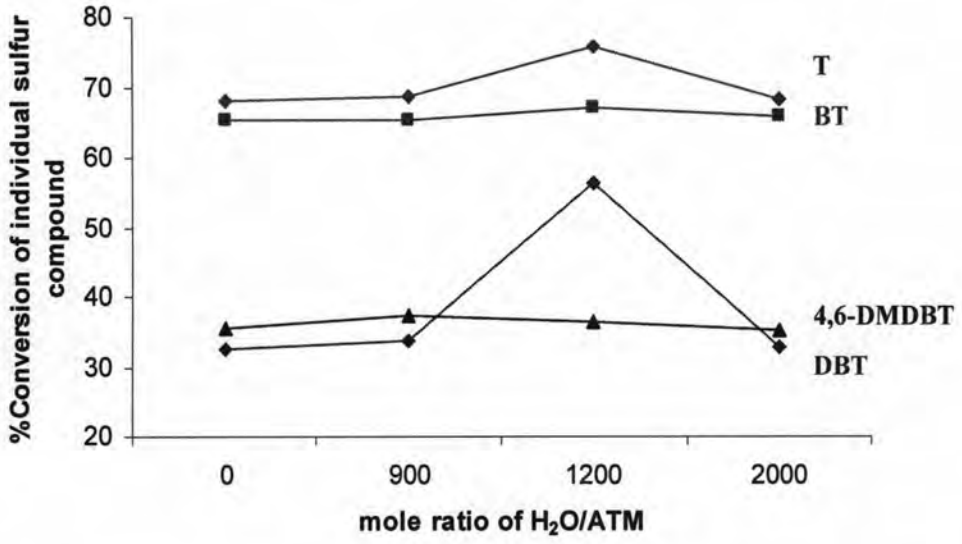

Figure 4.27 %Conversion of individual sulfur compounds in light cycle oil (LCO) using *in situ* generated MoS_2 catalyst from ATM with added water.

The %conversion of the individual sulfur compounds in LCO after the HDS reaction presented on Figure 4.27, it was shown that the reactivities each sulfur species decreased in the order: T > BT > DBT > 4,6-DMDBT. The order of reactivity similar in the most literatures. The possible explanation may be because that the various component of light cycle oil is less than straight run gas oil which is first distillation of crude oil.

Therefore, from the results obtained in this work, it was demonstrated that the *in situ* generated MoS_2 catalyst from ATM+H_2O can catalyze the HDS reaction of oil feedstocks at 350 °C, 30 atm H_2 for 2 h. and can reduce sulfur content of SRGO from 6100 ppmS to 3250 ppmS and from 310 ppmS to 100 ppmS for LCO at the molar ratio of H_2O/ATM about 1200.